



Article

Fucanases Related to the GH107 Family from Members of the PVC Superphylum

Jessica A. Gonzalez ¹, Nora M. A. Ponce ², Mariana Lozada ¹, Yasmín Daglio ², Carlos A. Stortz ² and Hebe M. Dionisi ¹,*

- Laboratorio de Microbiología Ambiental (CESIMAR-CONICET/IBIOMAR-CONICET), 2915 Puerto Madryn, Argentina; jgonzalez@cenpat-conicet.gob.ar (J.A.G.); lozada@cenpat-conicet.gob.ar (M.L.)
- Departamento de Química Orgánica, Facultad de Ciencias Exactas y Naturales, Ciudad Universitaria UBA, 1428 Buenos Aires, Argentina; aponce@qo.fcen.uba.ar (N.M.A.P.); ydaglio@qo.fcen.uba.ar (Y.D.); stortz@qo.fcen.uba.ar (C.A.S.)
- Correspondence: hdionisi@cenpat-conicet.gob.ar; Tel.: +54-280-488-3184

Abstract: The glycoside hydrolase 107 (GH107) family includes fucanase enzymes from only two bacterial phyla, Bacteroidota and Pseudomonadota. The goal of this work was to explore the diversity of putative fucanase enzymes related to this family in organisms of the PVC superphylum (Planctomycetota, Verrucomicrobiota, Chlamydiota), in order to expand our knowledge of the fucoidan-degrading potential in this ecologically and biotechnologically relevant group. Using hidden Markov modeland peptide-based annotation tools, 26 GH107 homolog sequences were identified in metagenome and genome datasets. The sequences formed two distinct clusters in a phylogenetic analysis, only one including members of the GH107 family. The endo-acting fucoidan degrading activity was confirmed in an enzyme included in the most divergent cluster. The fucanase, which probably originated in an uncultured planctomycete from the sampled subantarctic sediments, was cloned and expressed in *Escherichia coli*. The enzyme catalyzed the rapid hydrolysis of internal glycosidic bonds of fucoidan from *Macrocystis pyrifera*, a macroalgae species abundant at the site. It was active in a wide range of temperatures (5–45 $^{\circ}$ C), salinities (9.5–861 mM NaCl), and pH values (4.5–9), mainly producing sulfated α -(1,3)-linked fuco-oligosaccharides of various lengths. The PVC superphylum represents a promising source of fucanase enzymes with various biotechnological applications.

Keywords: fucoidanase; fucoidan; brown algae; Macrocystis pyrifera; glycoside hydrolase; C-PAGE



Citation: Gonzalez, J.A.; Ponce, N.M.A.; Lozada, M.; Daglio, Y.; Stortz, C.A.; Dionisi, H.M. Fucanases Related to the GH107 Family from Members of the PVC Superphylum. *J. Mar. Sci. Eng.* **2024**, *12*, 181. https:// doi.org/10.3390/jmse12010181

Academic Editors: Xue-Wei Xu, Lin Xu and Bin Wei

Received: 4 December 2023 Revised: 23 December 2023 Accepted: 10 January 2024 Published: 18 January 2024



Copyright: © 2024 by the authors. Licensee MDPI, Basel, Switzerland. This article is an open access article distributed under the terms and conditions of the Creative Commons Attribution (CC BY) license (https://creativecommons.org/licenses/by/4.0/).

1. Introduction

The Planctomycetota, Verrucomicrobiota, Chlamydiota (PVC) superphylum includes, in addition to the mentioned phyla, the Lentisphaerota and Kiritimatiellota phyla, as well as the Omnitrophota, Auribacterota, and Abyssubacteria candidate phyla. Organisms from this superphylum are recognized for their unique features, biotechnological potential, and human health or environmental relevance [1]. These phyla remain largely understudied, as only a small fraction of the diversity observed by culture-independent methods is currently represented in axenic cultures, or they are yet to have cultured representatives [2-4]. Members of this superphylum are particularly abundant in the marine environment, where they are proposed to play key ecological roles, such as in global nutrient cycling [5–7]. They have also been found associated with brown algae within their epiphytic biofilms [8–10], where algae exudates may influence the microbial community structure [10,11]. Despite the limited information on the metabolic potential of members of the PVC superphylum, recent studies have suggested that this group includes many members specialized in the degradation of sulfated polysaccharides synthesized by macroalgae [4,12,13]. Consequently, this taxon could be a promising source of enzymes targeting sulfated polysaccharides synthesized by macroalgae for various biotechnological applications.

Fucoidans are fucose-rich sulfated polysaccharides synthesized by brown algae and some marine invertebrates, which can include other monomers, such as galactose, glucose, xylose, mannose, and uronic acids, as well as acetyl groups [14]. Glycosidic linkages between α -L-fucopyranose residues can be either (1 \rightarrow 3), or both (1 \rightarrow 3) and (1 \rightarrow 4), with the sulfate groups substituting the O-2, O-3, and/or O-4 positions of the fucose. Brown algae fucoidans are highly heterogeneous regarding their branching patterns, monomeric composition, sulfate and acetate contents, and glycosidic linkages, characteristics that vary widely among species, seasons, and geographic locations, among other factors [14,15]. The complex and variable structures of fucoidans represent a barrier to their assimilation by marine microorganisms, requiring the action of various enzymes including endo- and exo-acting glycoside hydrolases (GHs) and debranching enzymes [4].

Enzymes that catalyze the hydrolysis of internal glycosidic bonds between α -L-fucopyranose residues are called fucanases (syn. fucoidanases) [16], currently included in the GH107, GH168, GH174, and GH187 families [17–20] of the Carbohydrate-Active enZymes (CAZy) database [21]. Compared to other GH families, which can contain thousands of members, these four families remain remarkably small. In particular, the GH107 family contains only 38 members from bacterial isolates of the Bacteroidota and Pseudomonadota phyla, from a candidate genome of a Gammaproteobacterium [22], and one member from the diatom *Thalassiosira oceanica* CCMP1005, according to the CAZy database (November 2023). Most of the characterized enzymes present endo- α -(1,4)-L-fucanase activity (EC 3.2.1.212) [17,22–27], while Mef2 from *Allomuricauda eckloniae* [28] and the enzymes Fda1 and Fda2 from *Alteromonas* sp. SN-1009 were reported as presenting endo- α -(1,3)-L-fucanase activity (EC 3.2.1.211) [29,30]. The majority of the members of the GH107 family present a complex and variable domain architecture, with only the (β/α)₈-barrel catalytic module (D1 domain) responsible for the fucanase activity being conserved among the members of the family [31,32].

Despite the ability of members of the PVC superphylum to assimilate fucoidans and their suggested specialization in the degradation of sulfated polysaccharides [4,13,33,34], very limited information is available on the fucoidan-degrading enzymes used by these organisms. In contrast to the other GH families including fucanases, no sequences from members of this superphylum are currently included in the GH107 family. In this work, we explored the diversity of sequences related to the GH107 family from members of the PVC superphylum, and we confirmed fucanase activity in a highly divergent enzyme from an uncultured planctomycete from intertidal sediments of a subantarctic environment, presenting a unique domain architecture.

2. Materials and Methods

2.1. Intertidal Sediment Metagenomic Datasets

Two metagenomic datasets from intertidal sediments of Ushuaia Bay (54°48′ S, 68°17′ W) were used for mining GH107 homolog sequences. More information about the sampling site and the experimental approach used for each metagenome dataset have been previously published [35,36]. Briefly, the OR07 dataset, containing 682,972 protein-coding sequences (CDSs), was generated by shotgun sequencing of a fosmid metagenomic library built from Ushuaia Bay intertidal sediments, and gene prediction was performed using MetaGeneMark v. 1 [37]. The MM metagenomic dataset (908,438 CDSs) was obtained by sequencing the sediments of a microcosm experiment where intertidal sediments of Ushuaia Bay were exposed to beached Macrocystis pyrifera blades retrieved from the same environment, followed by the assembly and gene prediction using the SqueezeMeta pipeline v1.5.1 [38] using Megahit v. 1.2.9 [39] and Prodigal v. 2.6.3 [40], respectively. Ushuaia Bay is exposed to multiple sources of pollution, including untreated domestic wastewater and chronic hydrocarbon pollution [41,42]. The NCBI accession numbers of the metagenomic sequences are, for the OR07 dataset OR545400-OR545405, PP035745-PP035748, and for the MM dataset OP559563, OP559567, OP559592, OP559602, OP559612, OP559618, OP559620, OP559626, OP559658, OP559666, OP559675, OP559678, OP559687, OP559696, OP559700,

OP559704, OP559706, OP559710, OP559726, OP559779, OP559780, OP559781, OP559808, OP559809, OP559816, OP559819, OP559833, OP559835, OP559845, OP559879, OP559907, OP559908, OP559910, OP559924, OP559926, OP559936, OP559938, OP559950, OP559960, OP559968, OP559981, OP559982, OP559987, OP559992, OP559993, and OR545406.

2.2. Identification of GH107 Homolog Sequences in Metagenomes, MAGs, and Genomes

The metagenomic datasets were annotated using the automated Carbohydrate-active enzyme Annotation (dbCAN2, https://bcb.unl.edu/dbCAN2/, 3 December 2023 [43]) and the Conserved Unique Peptide Patterns (CUPP, https://cupp.info/, 3 December 2023 [44]) tools. The NCBI non-redundant (NR) database [45] and the Integrated Microbial Genomes and Microbiomes system (IMG/M, https://img.jgi.doe.gov/, 3 December 2023 [46]) were searched with the Basic Local Alignment Search Tool alignment tool (BLAST, https://blast.ncbi.nlm.nih.gov/Blast.cgi, 3 December 2023 [47]), using the deduced amino acid sequences identified in the metagenomes as query and the blastp algorithm. Deduced amino acid sequences from genomes of members of the PVC superphylum were downloaded from the IMG/M system (February 2023). Putative GH107 sequences were identified in the genomes using two Hidden Markov Models (HMMs) built with the sequences of all the members of the GH107 family (February 2023), as well as with sequences identified in the metagenomes and by BLASTp searches (HMMER package v3.3.2 [48]).

2.3. Taxonomic Classification

The taxonomic assignment of the putative GH107 sequences was performed using the MEtaGenome ANalyzer software (MEGAN v. 6.24.19 with file megan-map-Feb2022 to map NCBI-nr accessions to taxonomy [49]) after the analysis of each metagenomic sequence using the blastp algorithm (10 October 2022) to retrieved the 100 closest matches, using default parameters [47]. The weighted lowest common ancestor (LCA) algorithm was chosen for the analysis, as it improves the specificity of the taxonomic assignment when compared with the naive LCA algorithm. In the case of scaffolds with at least five predicted coding sequences (CDSs), each sequence was analyzed using the same methodology (20 December 2023), and expressed as percentage of sequences assigned to a specific taxon. The taxonomic assignments were based on the NCBI taxonomy [50].

2.4. Sequence Similarity Network

The Sequence Similarity Network (SSN) was built using the Enzyme Similarity Tool (EFI-EST, https://efi.igb.illinois.edu/efi-est/, 3 December 2023 [51]), and included sequences from members of the GH107 family and putative GH107 sequences identified in sediment metagenomes and genomes of members of the PVC superphylum. The SSN was finalized using an alignment score of 25, which was found to generate subclusters that were in agreement with clades observed in previous phylogenetic analyses [20]. The SSN was visualized in Cytoscape v. 3.9.1 (https://cytoscape.org/, 3 December 2023 [52]).

2.5. Phylogenetic Analysis

Multiple sequence alignments were performed in ClustalW [53] in Jalview Version 2.11.2.6 (https://www.jalview.org/, 3 December 2023 [54]). The maximum likelihood phylogenetic tree was built in MEGA11 (https://www.megasoftware.net/, 3 December 2023 [55]), using the best model for the alignment as determined in MEGA11 (WAG + G), with 1000 bootstrap replicates.

2.6. In Silico Structural Analyses

The prediction of signal peptides was performed in the SignalP 6.0 (https://dtu.biolib.com/SignalP-6, 3 December 2023 [56]) and DeepTMHMM (https://dtu.biolib.com/DeepTMHMM, 3 December 2023 [57]) servers. InterproScan (https://www.ebi.ac.uk/interpro/, 3 December 2023 [58]) and CDD batch search (https://www.ncbi.nlm.nih.gov/Structure/, 3 December 2023 [59]) were used to annotate the domains contained in the

putative GH107 sequences. In addition, three-dimensional modeling was used to determine the number and the sequence range of the domains. The sequences were modeled in AlphaFold2, using ColabFold v1.5.2 [60]. The rank 1 model of each sequence was visualized in ChimeraX v. 1.4 [61]. Each domain was selected in ChimeraX, saved, and analyzed using the PDB search function in the DALI server (http://ekhidna2.biocenter.helsinki.fi/dali/, 3 December 2023 [62]). The structure of the top hits was analyzed to assess the potential function of the domains. In addition, the pairwise structure comparison function was used to compare two models or a model and a structure in the same server.

Sequence conservation analyses were performed in the ConSurf web server (https://consurfdb.tau.ac.il/, 3 December 2023 [63]. First, the sequence alignments were performed in ClustalWS [53] in Jalview Version 2.11.2.6 [54], and the selected region of the alignment was saved as an AMSA file. Both a selected model or structure in pdb format and the AMSA file were used to run the analysis using the default parameters (Bayesian calculation method and best evolutionary substitution model). The surface electrostatic potential of models and structures was calculated using the Poisson–Boltzmann equation in eF-surf (https://pdbj.org/eF-surf accessed on 4 October 2023).

2.7. Cloning, Recombinant Expression, and Purification of a Putative Fucanase

The full-length OR07_113643 gene without the signal peptide (residues Glu19-Gln394) was amplified by polymerase chain reaction (PCR) using a high-fidelity polymerase (Fast-Start High Fidelity PCR System, dNTPack, Roche Applied Sciences, Mannheim, Germany). Primers (OR07_113643_F 5'-CGATACATATGGAAGAGCCTCGCGTCTGG-3' and OR07_113643_R 5'-CACTACTCGAGCTACTGTTTTCTACTTTTCTTGACGG-3') were designed in Serial Cloner v 2.6.1. software (Franck Perez, Serialbasics) and synthesized in Integrated DNA Technologies, Inc. (Coralville, IA, USA). DNA was purified from the fosmids of the OR07 metagenomic library (QIAprep Spin Miniprep Kit, Qiagen, Inc., Valencia, CA, USA), and used as the template for the amplification of the putative fucanase gene. PCR products were digested with NdeI and XhoI restriction enzymes (Promega, Madison, WI, USA), purified, and cloned into the pET28-TEV vector (pET-28a(+), Novagen, Madison, WI, USA, modified with a TEV protease cleavage site, kindly provided by Dr. Rodolfo Rasia, IBR, Rosario, Argentina) fused to an N-terminal (N-term) histidine tag. The sequence fidelity was confirmed by DNA sequencing (Macrogen, Seoul, South Korea). Escherichia coli BL21 (DE3) cells (Novagen, Madison, WI, USA) transformed with the pET28-TEV-OR07_113643 construct were grown in 4xYT medium (32 g tryptone, 20 g yeast extract, 5 g NaCl per L) containing 50 μg/mL kanamycin (Sigma-Aldrich, St Louis, MO, USA), at 12 °C and 200 rpm until OD_{600 nm} of 6. An aliquot of the initial culture was inoculated into the same medium (OD $_{600 \text{ nm}}$ 0.1) and grown in the same conditions until OD $_{600 \text{ nm}}$ 0.8, where the protein expression was induced with 0.2 mM isopropyl β-D-thiogalactopyranoside (IPTG, Thermo Scientific, Waltham, MA, USA), or 1% (w/v) glucose (Merck Life Science, Darmstadt, Germany) was added as a control. Growth continued for 19 h additional hours in the same conditions, where OD_{600nm} was 2.2.

The cultures were harvested by centrifugation at $5000 \times g$ for 10 min at 4 °C. The bacterial cells were washed and suspended in 100 mM Tris-HCl (pH 7.5), 500 mM NaCl, 0.2 mM PMSF, 10% (v/v) glycerol, and 5 mM sodium imidazole. The cells were disrupted with Fastprep-24TM (MP Biomedicals, CA, USA) for two cycles of 4 m/s for 10 s, with 5 min on ice between cycles. The cell lysate was centrifuged at $11,600 \times g$ for 10 min at 4 °C, and the supernatant was loaded onto a nickel-affinity chromatography column (Ni-NTA agarose, Invitrogen, Carlsbad, CA, USA) equilibrated with 100 mM Tris-HCl (pH 7.5), 500 mM NaCl, 10% (v/v) glycerol and 5 mM sodium imidazole. The His-tagged proteins were eluted with 100 mM Tris-HCl pH 7.5, 500 mM NaCl, 10% glycerol, and 300 mM sodium imidazole. Fractions containing the target proteins were identified by SDS-PAGE [64], dialyzed at 5 °C in 100 mM Tris-HCl pH 8, 500 mM NaCl, 10% (v/v) de glycerol, and concentrated using a Vivaspin filter unit (MWCO 3 kDa, GE Healthcare UK

Ltd., Little Chaltont Buckinhamshire, UK). The purified protein was quantified [65] and stored at -20 °C after the addition of 5% (v/v) glycerol.

2.8. Fucoidan Purification and Characterization

Samples of M. pyrifera (Phaeophyceae, order Laminariales) were collected in Bahía Camarones (S 44°46.57′, W 65°34.47′) Chubut, Argentina. Sixty grams of dried blades (BL), gas bladders (GB), or stipes (ST) were milled and extracted with methanol/chloroform/water (4:2:1) at room temperature for 24 h. The residue was recovered after filtration through 2.7 µm glass microfiber filters (M6-D, 47 mm in diameter, Munktell, Grycksbo, Sweden) and dried for 24 h at room temperature. Subsequently, two sequential extractions were applied, first with 80% (v/v) ethanol at room temperature for 24 h, and then at 70 °C for 7 h. The next step consisted of treatment with 0.01 M HCl (pH 2) for 6 h at room temperature to yield the fucoidans. The supernatant was recovered by centrifugation, neutralized, dialyzed (MWCO 6–8 kDa, Spectra/Por[®], Spectrum Laboratories, Rancho Dominguez, CA, USA), and lyophilized. The obtained yield was 6, 5.5, and 3% on a dry weight basis for BL, GB, and ST, respectively. Total carbohydrates were estimated by phenol-sulfuric acid method using fucose as standard [66]. Uronic acids were determined using the method of Filisetti-Cozzi and Carpita [67] using glucuronolactone (Sigma-Aldrich, Saint Louis, MO, USA) as standard. The BaCl₂-gelatin method was used to determine the sulfate content, after hydrolysis with 1 M HCl at 110 °C for 4.5 h, using Na₂SO₄ as the standard [68]. After hydrolysis (2 M trifluoroacetic acid for 90 min at 121 °C), neutral sugars were derivatized to the acetylated alditols and quantified by gas chromatography (GC) using a capillary column $(30 \text{ m} \times 0.25 \text{ mm})$ coated with SP-2330 $(0.20 \text{ }\mu\text{m})$ on a Nexis GC-2030 (Shimadzu, Kyoto, Japan) with a flame ionization detector (FID). Nitrogen was used as the carrier gas, with a flow rate of 1 mL/min and a split ratio of 100:1. Chromatography runs were isothermal at 220 °C, while the injector and detector were set at 240 °C. The anionic polysaccharides were precipitated with a 10% (w/v) aqueous solution of hexadecyltrimethylammonium bromide (cetrimide, Sigma-Aldrich, Saint Louis, MO, USA), and sequentially redissolved according to their ionic charge with increasing NaCl concentrations (0.5, 1, 2, and 3 M), yielding the fractions F1BL, F2BL, F3BL, and F4BL, respectively.

BL and F4 from BL were analyzed by gel permeation chromatography (GPC) in a HPLC system (Shimadzu, Kyoto, Japan) equipped with an LC-20AT pump, a refractive index detector (Model RID-10A), and two columns connected in series: Waters Ultrahydrogel 250 (300 \times 7.8 mm) and Waters Ultrahydrogel 120 (300 \times 7.8 mm) (Waters Corporation, Milford, MA, USA). A solution of 0.05 M NaNO $_3$ and 0.02% NaN $_3$ was used as the mobile phase. The column was calibrated using dextran standards of different MWs (31.5, 53, 66, 134, and 410 kDa, Sigma-Aldrich [Saint Louis, MO, USA] and American Polymers Standards [Mentor, OH, USA]).

Fucoidan from *Undaria pinnatifida* sporophylls was extracted using the same methodology used for *M. pyrifera*. Fucoidans from *Adenocystis utricularis, Scytosiphon lomentaria* were obtained previously [69,70]. Fucoidans from *Myriogloea major, Eudesme virescens, Colpomenia sinuosa*, and *Asperococcus ensiformis*, kindly provided by Ezequiel Latour, were purified as previously reported [71,72].

2.9. Fucanase Activity

Fucanase activity was monitored by carbohydrate-polyacrylamide gel electrophoresis (C-PAGE) [16]. The reaction mixture contained 100 mM Tris-HCl (pH 7.5), 500 mM NaCl, 0.4% (w/v) fucoidan, and 1 μ M of the enzyme, except when otherwise indicated. The enzymatic reaction was incubated at 25 °C for 25 min, stopped by heating at 80 °C for 5 min, and electrophoresed at 20 mA in a 27% (w/v) 29:1 acrylamide/bis-acrylamide gel with 40 mM Tris-HCl buffer (pH 7.8) (Sigma-Aldrich, St. Louis, MO, USA) and 40 mM acetic acid (Merck Life Science, Darmstadt, Germany), for 4 h. Gel staining was performed in 0.03% (w/v) alcian blue 8 GX in 2% (v/v) acetic acid or 0.1% (v/v) o-toluidine blue (Sigma-Aldrich, St. Louis, MO, USA) for 10 h at room temperature. Gel destaining was

performed in 1% (v/v) acetic acid (Merck Life Science, Darmstadt, Germany). The fucanase activity was also tested at different temperatures (5 to 65 °C) for 30 s and 1 min, at different pH values (2.5, 3.5, 5.5: 100 mM PIPES, 4.5: 100 mM sodium acetate, 6.5: 100 mM HEPES, 7.5, 8, 8.5, 9: 100 mM Tris-HCl, 10: boric acid/KCl) at 25 °C for 25 min, and at different NaCl concentrations (10–1300 mM) at 25 °C for 25 min.

2.10. Preparation and Characterization of Enzymatic Products

The BL fucoidan (0.2 g) was dissolved in 15 mL of 100 mM Tris-HCl buffer (pH 7.5), with 300 mM NaCl and 0.6 mg of fucanase OR07_113643. The reaction mixture was incubated at 25 °C for 70 h with mixing at 60 rpm, and the enzymatic reaction was stopped at 80 °C for 10 min. High molecular weight products (HMWP) were precipitated with 1:3 (v/v) ethanol and separated by centrifugation at $9000 \times g$ for 20 min. The supernatant containing the low molecular weight products (LMWP) was evaporated under vacuum to remove the alcohol, diluted with distilled water, and separated in a Bio-Gel P-6 column (1.5 × 90 cm, Bio-Rad, Hercules, CA, USA) equilibrated with water. Fractions were analyzed by the phenol-sulfuric method [66], and those containing LMWP were applied to a Bio-Gel P-2 column (1.5 × 73 cm, Bio-Rad, Hercules, CA, USA) and freeze-dried. The eluted fractions (F1-P2 and F2-P2) were recovered and freeze-dried.

The F1-P2 fraction was analyzed by GPC as described in item 2.9. Monosaccharide composition was determined using GC as previously described, and the sulfate content was determined by ion chromatography (DIONEX DX-100, Dionex Corp., Sunnyvale, CA, USA). For NMR analysis, 12 mg of the F1-P2 fraction was dissolved in 0.8 mL of D₂O and analyzed in a Bruker Avance Neo spectrometer (Bruker, Billerica, MA, USA), at a frequency of 500.13 MHz (1 H) and 125.77 MHz (13 C), at room temperature. Acetone was used as an internal standard, calibrating the methyl group to 2.22 ppm in 1 H and 31.1 ppm in 13 C. The analysis by mass spectroscopy (MS) was performed using a BrukerMicrOTOF-Q II (Bruker Daltonics, Billerica, MA, USA) equipped with electrospray (ESI) in negative ion mode.

3. Results

3.1. Diversity of GH107 Homolog Sequences in Intertidal Sediment Metagenomes

Sequences homologous to members of the GH107 family were identified in two metagenomic datasets from intertidal sediments of a subantarctic environment, named MM [35] and OR07 [36] (see details in Section 2). The two tools used for the annotation, dbCAN2 and CUPP [43,44], produced similar results (Table S1). The two annotation tools identified fifty-two sequences as related to the GH107 family, six from the OR07 dataset, and forty-six from the MM dataset. The taxonomic assignment of the identified protein coding sequences (Megan6, [49]) suggested they could belong to organisms from the Bacteroidota, Pseudomonadota (Gammaproteobacteria class), and Planctomycetota phyla, with only one sequence not classified at the phylum level (Table S2). The taxonomic assignment of the scaffolds was determined as the consensus of the assignment of each of the sequences predicted in scaffold with at least five CDSs. The assignment of the putative GH107 sequence and the scaffold containing the sequence were in agreement at the phylum or superphylum level (Table S2).

A Sequence Similarity Network (SSN) was used to explore the diversity of sequences identified in the metagenomic datasets, relative to the current diversity of members of the GH107 family (both characterized and uncharacterized). A SSN graphically represents a collection of pairwise alignments between homologous sequences (or nodes), where only those that have a score above a user-defined similarity cut-off are connected by lines (or edges) [73]. In the network, the most closely related sequences can be visualized as clusters of connected nodes. The SSN included the sequences identified in the intertidal sediment metagenomes, their two closest matches in the NCBI NR protein database (BLASTp algorithm) (Table S2), and the members of the GH107 family (dataset of November 2023). Using a cutoff value of 25, all but one of the members of the GH107 family appeared organized in a large cluster, divided into three distinct subclusters (Figure 1, subclusters A, B and C).

The only sequence from the GH107 family not included in this cluster is WGE89193 from *Actinobacillus arthritidis*, which is a singleton in the network. Two of the subclusters also contained the majority of the identified metagenomic sequences and their closest matches (subclusters A and B). On the other hand, one metagenomic sequence formed a small cluster with two sequences identified with BLASTp searches, and one metagenomic sequence was a singleton. The latter is the case of the partial sequence OR07_27010, assigned to the Planctomycetota phylum, which shared low sequence identity values with the closest sequences from the NCBI database (Table S2).

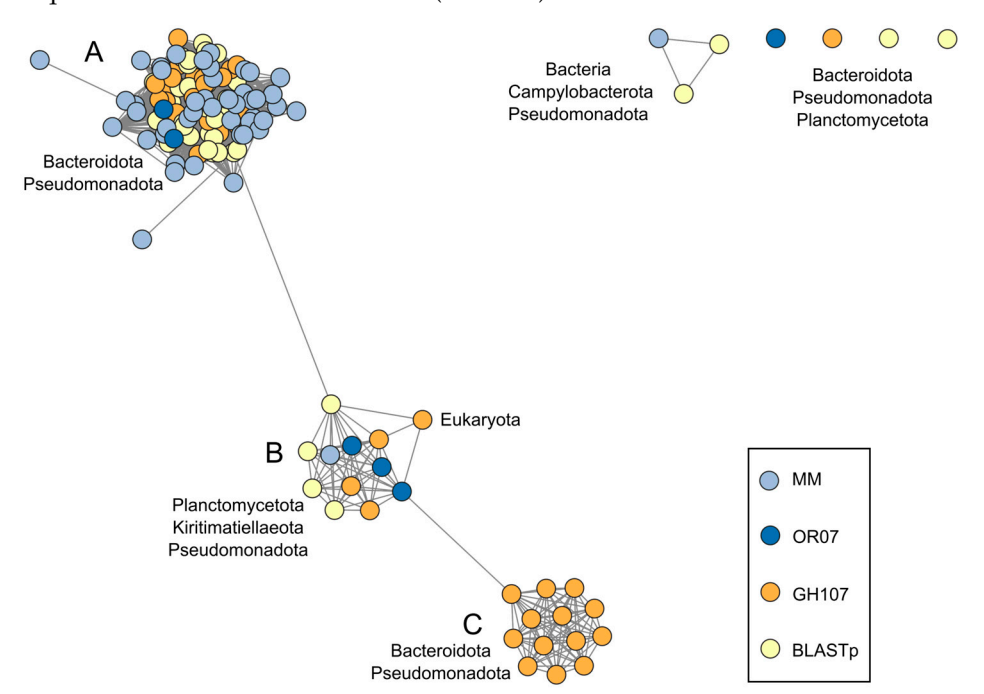


Figure 1. Sequence Similarity Network (SSN). The SSN was built using the Enzyme Function Initiative-Enzyme Similarity Tool (EFI-EST, alignment score 25). The network includes sequences of the GH107 family (orange nodes), GH107 homolog sequences identified in the sediment metagenomes (OR07, dark blue nodes; MM, light blue nodes), and the two top hits identified using the BLASTp algorithm against the NCBI non-redundant (NR) database with the metagenomic sequences as query (light yellow nodes). The phylum or domain of the organisms where the sequences were identified, or the taxonomic assignment of the GH107 homolog sequences, are indicated next to each cluster/subcluster or group of singleton sequences. The accession number and organism of the sequences included in each cluster, as well as the metagenomic sequence IDs, can be found in Table S3.

Subcluster A of the SSN included sediment sequences assigned to the Bacteroidota and Pseudomonadota (Gammaproteobacteria class) phyla, as well as sequences of the GH107 family and sequences from the NCBI NR database identified in genomes from members of these phyla (Table S3). Subcluster B, on the other hand, included sequences identified in the metagenomic datasets assigned to the Planctomycetota phylum, as well as their closest matches, which were identified in members of the PVC superphylum (Figure 1, Table S3). The sediment sequences and their closest matches from the NCBI database often shared high identity values at the amino acid level (Table S2). Subcluster B also included three sequences of the GH107 family from two members of the Alteromonadales order of the Gammaproteobacteria, *Alteromonas* sp. SN-1009 (NCBI accession numbers AAO00508 and AAO00509) and *Shewanella violacea* DSS12 (BAJ00350), and one sequence from the eukaryotic organism *T. oceanica* CCMP1005 (JGI 72602), recently included in the GH107 family. Subcluster C contained sequences of the GH107 family, identified in members of the Bacteroidota and Pseudomonadota phyla and from an uncultured bacterium probably belonging to the Gammaproteobacteria class [22].

3.2. GH107 Homolog Sequences from Members of the PVC Superphylum

3.2.1. Sequence Identification

The SSN (Figure 1) suggested that sequences from members of the Planctomycetota and Kiritimatiellaeota phyla (both included in the Planctomycetota, Verrucomicrobiota, and Chlamydiota (PVC) superphylum) could be related to members of the GH107 family, which could expand the current taxonomic diversity of organisms containing these genes. To further explore the diversity of sequences related to the GH107 family in members of the PVC superphylum, we searched genomes from members of the PVC superphylum using HMMs constructed from an alignment of the D1 region (putative catalytic domain) of bacterial sequences included in subcluster B of the SSN (Figure 1). Similar results were obtained with an HMM built using an alignment of the D1 region of 34 sequences of the GH107 family from the CAZy database (accessed February of 2023). All sequences identified in BLASTp searches sharing >60% identity at the protein level with the sediment sequences assigned to the Planctomycetota phylum were also included in the dataset for further analyses. The identified sequences were further annotated using the dbCAN2 and CUPP servers [43,44] in order to assess their relationship with the GH107 family (Table S4). Only sequences with the lowest e-values ($<10^{-35}$) in the identification resulted in the annotation by these servers as members of the GH107 family. The most common unspecific identifications, eliminated from further analyses, were sequences related to the GH29 family (α -L-fucosidases), as these families are structurally related [31]. The genomes have been annotated by the CAZy database but the catalytic modules from the identified sequences were not included in the GH107 family, suggesting that they did not meet the requirements of the database for their annotation.

3.2.2. Phylogenetic Relationships

A phylogenetic analysis was performed including the D1 (catalytic) domain of sequences of the GH107 family and GH107 homologs from members of the PVC superphylum, in order to assess the relationships among these sequences. Although only a portion of the sequences were included in both analyses, there was a partial agreement between the grouping in the SSN (Figure 1) and the phylogenetic tree (Figure 2). In particular, sequence WGE89193 from *Actinobacillus arthritidis*, a singleton in the SSN, did not cluster with the rest of the sequences of the GH107 family. In addition, a cluster of the phylogenetic tree (Figure 2, cluster A) included the same GH107 sequences as subcluster A of the SSN (Figure 1, Table S3). These sequences were identified in various members of the Bacteroidota and Pseudomonadota phyla, such as strains of the *Polaribacter* and *Psychromonas* genera. Sequence identity in the D1 domain for sequences in this cluster ranged from 34.1 to 99.7%. None of the identified putative GH107 sequences from members of the PVC superphylum clustered with these sequences.

The second branch of the phylogenetic tree included sequences from subclusters B and C of the SSN. The larger and well-supported cluster contained the 12 GH107 members from subcluster C of the SSN, including sequences from *Wenyingzhuangia fucanilytica, Mariniflexile fucanivorans, Formosa* spp., *Flavobacterium algicola*, and an uncultured gammaproteobacterium (Figure 2 cluster C). This cluster also included 11 GH107 homolog sequences identified in genomes of members of the PVC superphylum. This cluster contained seven sequences (CAA6677129, CAA6677969, CAA6677966, CAA6677968, CAA6677967, CAA6678285, and CAA6678994) identified in the genome of *Lentimonas* sp. CC4 (Verrucomicrobiota phylum). In addition, cluster C included sequences identified in *Pontiella* spp. (Kiritimatiellaeota phylum), as well as in *Novipirellula aureliae* and *Rhodopirellula lusitana* (Planctomycetota phylum). Protein sequence identities in the D1 region among the sequences from cluster C ranged between 33.8 and 89.3%.

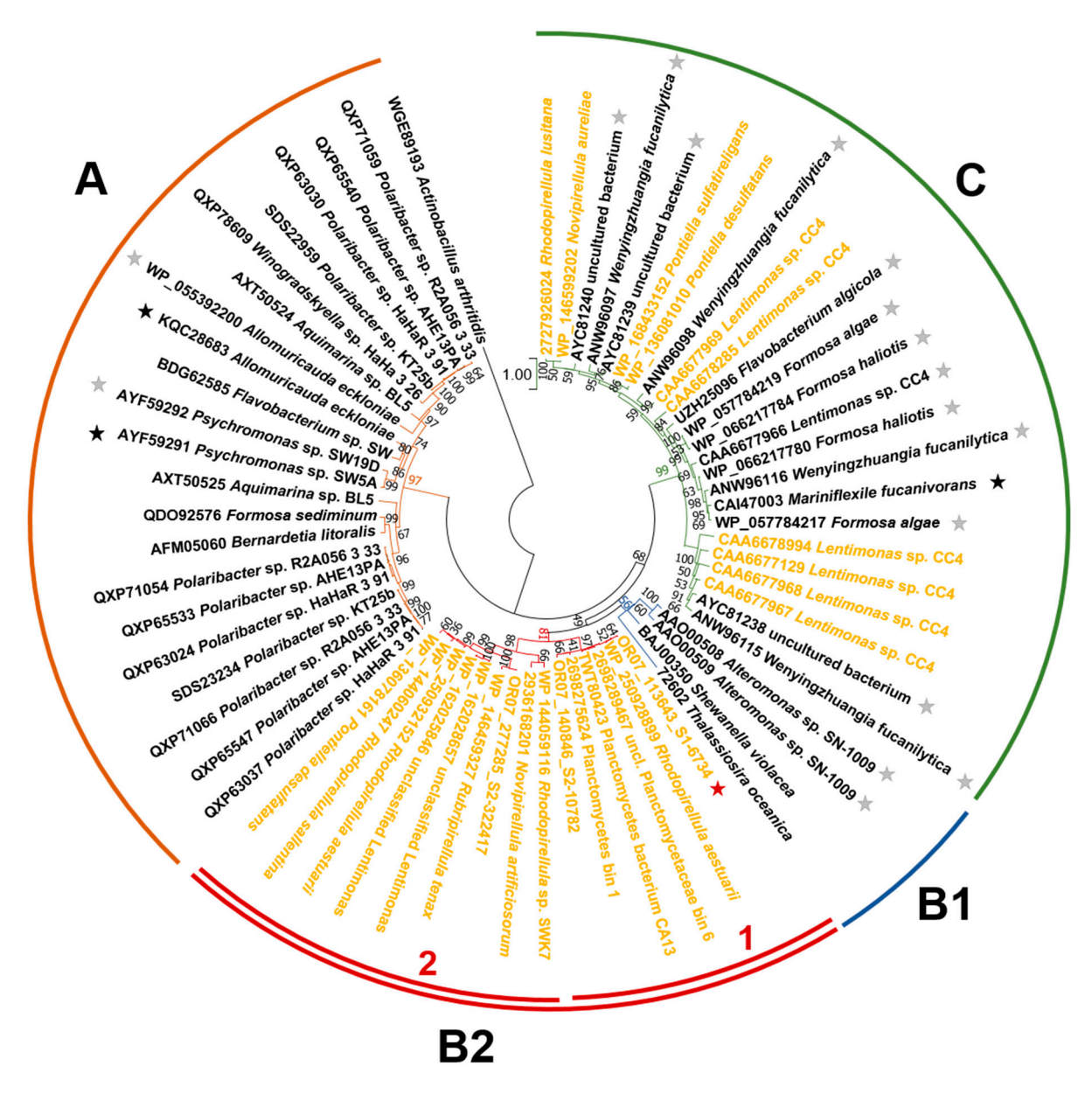


Figure 2. Phylogenetic analysis of the D1 domain of GH107 homolog sequences from members of the PVC superphylum. Sequences identified in genomes from members of the PVC superphylum or in the OR07 sediment metagenome are indicated in gold font, sequences from the GH107 family are indicated in black font. Letters and line colors indicate clusters of the tree. Gray stars indicate previously characterized enzymes, black stars enzymes with determined three-dimensional structure, and a red star the enzyme characterized in this work. The D1 domain was aligned in ClustalW version 2.1 [53] in Jalview 2.11.2.6 [54], and a maximum likelihood unrooted phylogenetic tree was constructed in MEGA 11 [55] using the WAG + G model, with 1000 repetitions.

Sequences included in subcluster B of the SSN (Figure 1) presented low support in the phylogenetic tree (Figure 2). GH107 sequences and sequences from organisms belonging to the PVC superphylum separated into two clusters, one including the sequences from the GH107 family from *S. violacea* DSS12, *Alteromonas* sp. SN-1009, and the diatom *T. oceanica* CCMP1005 (cluster B1), and the second cluster including GH107 homolog sequences identified in members of the Planctomycetota, Verrucomicrobiota, and Kiritimatiellota phyla (cluster B2). Within the latter, two subclusters with high support were observed. Subcluster 1 included the metagenomic sequences OR07_113643 and OR07_140846, and sequences from genomes and MAGs from PVC bacteria (Planctomycetes bacterium CA13,

TWT80423; Kelp biofilm-associated Planctomycetes bin 1, IMG/M system ID 698275624; unclassified Planctomycetaceae bin 6, IMG/M system ID 2698289467; *Rhodopirellula aestuarii*, WP_250928899). Sequence identities at the protein level in subcluster 1 ranged between 75 and 87%.

Subcluster 2 included sequence OR07_277285 from subantarctic sediments, as well as sequences identified in genomes of PVC superphylum members: *Rubripirellula tenax*, (WP_146459327), *Pontiella desulfatans* (WP_136078161), *Rhodopirellula tenax* (WP_144060247), *Rhodopirellula aestuarii* (WP_250932152), *Novipirellula artificiosorum* Poly41 (IMG/M ID 2936168201), *Rhodopirellula* sp. SWK7 (WP_144059116), and unclassified Lentimonas (WP_162028657 and WP_162025846). Sequence identities in subcluster 2 ranged from 51 to 99%.

The sequences from PVC members of cluster C of the phylogenetic tree were annotated as belonging to the CUPP groups GH107:1.1 or GH107:3.1 (Table S4). Sequences from cluster B2 subcluster 1 (with the exception of those from the OR07 metagenomic dataset), as well as the sequence WP_136078161 from *P. desulfatans* from cluster B2 subcluster 2 were included in CUPP group GH107:4.1. These groups, defined by the CUPP annotation tool, include members of the GH107 family as well as sequences from the NCBI database from members of the PVC superphylum.

The results of the phylogenetic analysis support the relationship between members of the GH107 family and GH107 homolog sequences from organisms of the PVC superphylum. In spite of the limited genome dataset, a high diversity of sequences related to members of the GH107 family was identified in organisms of the PVC superphylum, with sequences included in cluster C of the phylogenetic tree more closely related to GH107 members than those from cluster B2.

3.2.3. In Silico Structural Analyses of the D1 Domain

While the inclusion of sequences from members of the PVC superphylum in cluster C of the phylogenetic tree showed high support, clustering with 12 GH107 members, the phylogenetic relationship of sequences from cluster B2 with members of this family showed more uncertainty (Figure 2). We analyzed the residue conservation in this group of sequences to shed light on their potential evolutionary relationships. Figure 3 A shows the residue conservation (ConSurf server analysis, [63]) of the 15 sequences of cluster B2, and bacterial sequences of the GH107 family included in the same subcluster of the SSN, from Alteromonas sp. SN-1009 (AAO00508 and AAO00509) and S. violacea DSS12 (BAJ00350). The conservation was mapped into the three-dimensional model of the D1 domain of sequence OR07_113643 (AlphaFold2, [60]). The analysis showed a high level of conservation in the putative active site, but conservation was also observed in some regions of the modeled α helices in the periphery of the molecule. An alignment showed a high level of residue conservation among the sequences from cluster B2 (Figure S1), including the positions of Asp226 proposed as catalytic nucleophile, His294 proposed as the general acid/base, and the -1 subsite residues Tyr147 and Trp351 (MfFcnA4 numbering, [31]). Other residues of the −1 subsite were not fully conserved, such as Asn149, replaced by Ala in sequences of subcluster 1 (and in GH107 sequences from Alteromonas sp. SN-1009 and S. violacea DSS12), or by Ser in part of the sequences from subcluster 2 (Figure S1). Although Asn is the residue most often found in this position, both Ala and Ser have previously been observed in this position in members of the GH107 family [28]. The -1 subsite residue Asn270 was mostly replaced by His.

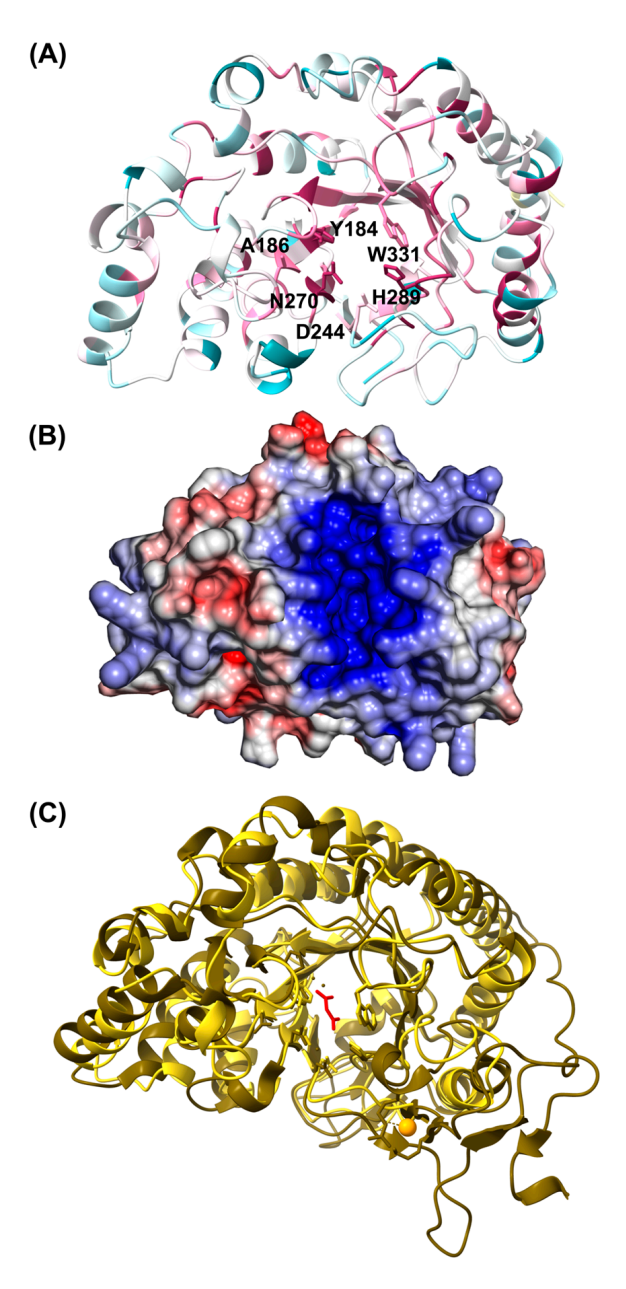


Figure 3. In silico analyses of the D1 domain. (**A**) Conservation of residues. Sequences included in the analysis: cluster B2 of the phylogenetic tree and sequences AAO00508, AAO00509, and BAJ00350 of cluster B1 (Figure 2). The reference is the three-dimensional model of the D1 domain of sequence OR07_113643 as a cartoon representation (AlphaFold2 using MMseqs2, ColabFold v1.5.2, [60]). Coloring indicates the level of conservation, from dark teal (less conserved) to dark purple (most conserved) (ConSurf server, [63]). Key residues of the active site are shown as sticks in the same color. Numbering corresponds to the sequence OR07_113643. (**B**) Surface electrostatic potential of the OR07_113643 model of the D1 domain. The view of the molecule with the groove of the putative active site is shown. The surface electrostatic potential was calculated by solving the Poisson–Boltzmann equation, with blue and red indicating positive and negative surface electrostatic potential, respectively. (**C**) Three-dimensional model of the D1 domain of sequence OR07_113643 (in yellow) superimposed to the structure of P5FcnA from *Psychromonas* sp. SW5A (6M8N, in brown). Key residues of the active site are shown as sticks in the same color. The malonate molecule bound to P5AFcnA is shown in red, and the Ca²⁺ atom is shown in orange. Model quality indicators can be found in Figure S9.

The putative active site of the D1 domain of OR07_113643 and other sequences from Cluster B2 showed a groove shape with a strong positive surface electrostatic potential (Figures 3B and S2). Similar characteristics have been reported in other fucanases of the GH107 family and are compatible with the binding of the negatively charged substrate [27,31]. The overall surface electrostatic potential, however, showed fewer negative charges, when compared to the enzymes MfFcnA4 from M. fucanivorans SW5 (pdb ID 6DLH) and P5FcnA from *Psychromonas* sp. SW5A (pdb ID 6M8N), but not Mef1 from A. eckloniae (pdb ID 8BPD) (Figure S2). The three-dimensional model of the D1 domain of sequence OR07_113643 shows an organization similar to the structure of P5FcnA from Psychromonas sp. SW5A, superimposing in residues 36 to 380 from P5FcnA with a similar secondary structure (Figure 3C). When comparing this structure and the model of sequence OR07_113643, the z-score was 36.6 and the root mean square deviation (RMSD) was 2.1 A over 301 residues, with 20% sequence identity (DALI web server, [62]). The main difference between the structure of P5AFcnA and the OR07_113643 model was the loop between Val261 and His233 of P5AFcnA that binds a Ca²⁺ molecule [31], which was missing in OR07_113643 (Figures 3C and S3A). A Ca²⁺ binding site identified in MfFcnA4 (Ca1, [31]), was also missing in the model of sequence OR07_113643 (Figure S3B).

The structural similarities between sequences from cluster B2 of the phylogenetic tree and members of the GH107 family, as well as the conservation of key residues of the active site, suggest that the putative enzymes could catalyze the hydrolysis of internal glycosidic bonds of the fucoidan molecules.

3.2.4. Domain Architecture

A signal peptide was detected in the full-length metagenomic sequences assigned to the Planctomycetota phylum (OR07_113643, OR07_140846, and OR07_277285) and in the majority of the sequences identified in genomes and MAGs of members of the PVC superphylum (Table S4), suggesting the secretion of these putative enzymes. This is in agreement with the endo-acting mechanism of enzymes of the GH107 family.

The GH107 homolog sequences from cluster B2 of the phylogenetic tree (Figure 2) were shorter than the sequences from cluster C, suggesting a less complex domain architecture in sequences of the more divergent cluster (Table S4). Metagenomic sequences OR07_113643 and OR07_140846, as well as the rest of the sequences from subcluster 1, contained an SLA1 homology domain 1 (SHD1, PF03983) at the N-term end, followed by a putative GH107 (D1) catalytic module (Table S5). An alignment of the region corresponding to the SHD1 domain from sequences of subcluster 1 with the cytoskeleton assembly control protein SLA1 from Saccharomyces cerevisiae (PDB ID 2HBP, [70]) and the putative cytoskeleton assembly control protein SLA1 from Rhodopirellula baltica SH 1 (CAD77399) showed a high level of sequence conservation (Figure S4A). Furthermore, the pairwise comparison of the model of OR07_113643 (without the signal peptide) with the structure 2HBP showed a similar fold (Figure S4B), a z-score of 10.2, and an RSMD of 1.3 Å, with 26% sequence identity over 58 residues (DALI server, [62]). The SHD1 domain has been proposed as specific for proteins of PVC bacteria [74]. In order to assess how abundant this domain was in genomes of members of the PVC superphylum, we searched for the PF03983 domain in their proteincoding sequences in the IMG/M system database [46]. The 45.5% of the genomes from the Planctomycetota, Verrucomicrobiota, and Kiritimatiellota phyla (998 genomes) contained sequences from various protein families with this domain, with an average of 2.7 copies per genome. The sequences from subcluster 2 of the phylogenetic tree were shorter and only contained a putative GH107 catalytic module (Tables S4 and S5).

The rest of the GH107 homolog sequences identified in members of the PVC superphylum, included in cluster C of the phylogenetic tree (Figure 2), presented a more complex domain architecture with the prediction of various domains (Table S5). Three-dimensional models were built in Alphafold2 [60] to define the potential boundaries of these domains, and each domain was further analyzed using the Dali server [62] to assess its potential function. The modeling of the spatial organization of the observed domains is, however,

not currently reliable [60]. All the sequences from cluster C (Figure 2), except the models of sequences CAA6677969 and CAA6678285 from *Lentimonas* sp. CC4, contained one or two domains similar to the Ig-like R1-R3 domains of MfFcnA from *M. fucanivorans* (CAI47003, [17]), in the same position next to the D1 domain (Table S5). Figure 4 shows the presence of conserved residues in both the D1 and R1 domains in sequences of cluster C (ConSurf server, [63]).

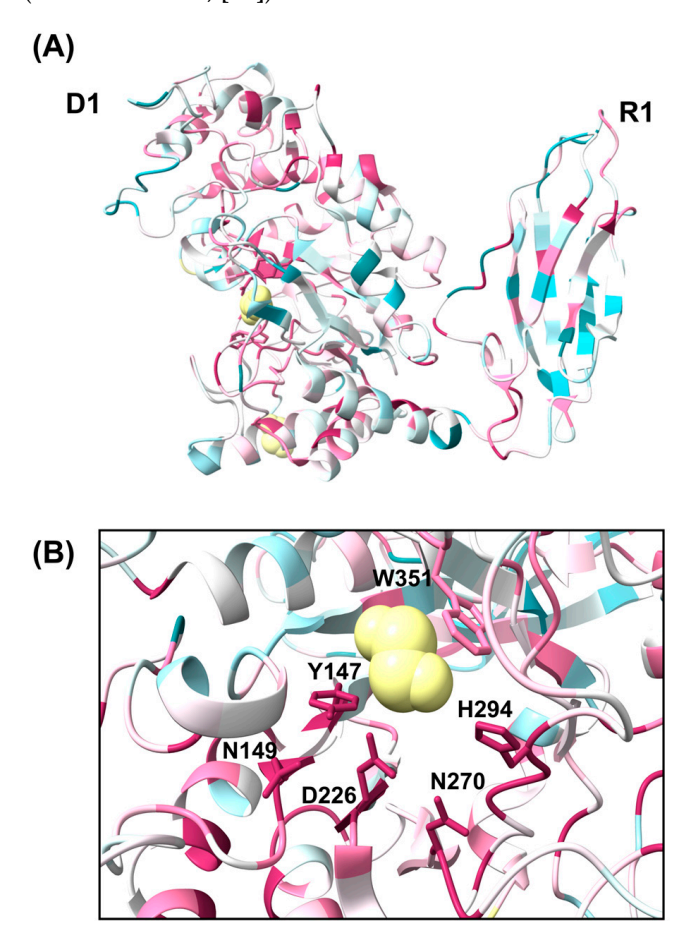


Figure 4. Conservation of residues in sequences included in cluster C (except sequences CAA6677969 and CAA6678285 from *Lentimonas* sp. CC4). (**A**) The conservation of the alignment in the D1-R1 domains (residues 36 to 513) was mapped in the structure of MfFcnA from *M. fucanivorans* (PDB ID 6DLH). Coloring indicates the level of conservation in the sequences, from dark teal (less conserved) to dark purple (most conserved) (ConSurf server, [63]). (**B**) Active site region showing key residues of the active site as sticks in the same color, with MfFcnA. Yellow, 1,2-ethanediol molecules of the 6DLH structure.

Another domain commonly found in sequences from cluster C from members of the PVC superphylum showed a similar fold to the structure of the Emp47p carbohydrate recognition domain (CRD) from *S. cerevisiae* (PDB ID 2A6Z and 2A6Y) (Table S5). Two putative CRD domains sharing 41% sequence identity were located at the N-term end of sequence CAA6678994. The analysis of this region in the Dali server indicated an RMSD 2.8 Å over 192 residues and 12% identity with structure 2A6Z (Figure S5). Sequence CAA6677129 from *Lentimonas* sp. CC4 contained one putative CRD domain in the N-term end of the protein (Table S5). Regions with unknown function at the N-term end of the fucanase Fp273 from an uncultured bacterium (AYC81238) and the enzymes FWf2 and FWf3 from *W. fucanilytica* [24] shared 41–42% sequence identity with the putative CRD domain from sequence CAA6677129. Sequences CAA6677966 and CAA6677969 also had a putative CRD domain, but in these sequences, they were located after the D1 domain (Table S5).

A domain annotated as Concanavalin A-like lectin/glucanase domain superfamily (IPR013320) and/or as Laminin_G_3 (PF13385) domain (CDD search, InterproScan) was located near the C-terminal (C-term) end of sequences CAA6677966, CAA6677967, CAA6677968, and CAA6678994 from *Lentimonas* sp. CC4 (Table S5). Sequence CAA6677967 had an additional domain with a similar fold, but it was not annotated by these tools. After the Concanavalin A-like module, the C-term end of the *Lentimonas* sp. CC4 sequences contained a 100-residue domain with a fibronectin type III-like fold that shared 37 to 85% sequence identity (named U1, Table S5). Sequences from *Pontiella* spp. (WP_136081010 and WP_168433152) also contained a domain with a similar fold at the C-term end (12-20% identity with the U1 region of *Lentimonas* sp. CC4 sequences). The two *Pontiella* spp. sequences also contained two additional domains with unknown functions, one at the N-term end and a second near the C-term end (named U2, Table S5), sharing 39 to 68% sequence identity. This domain had a fold similar to the structure of a DUF4465 family protein from Bacteroides caccae ATCC 43185 (4JQR, Dali server, RMSD 3.2 Å, 140 residues, 10% identity), and to the conserved all β-strand domain of MfFcnA (Alphafold2 model, UniProt ID Q08I46).

A ricin B lectin 2 domain (PF14200) was detected in sequence CAA6678285 from *Lentimonas* sp. CC4 (Table S5). This region of the protein was annotated in the dbCAN2 server as belonging to the CBM13 family and showed a modeled structure similar to the CBM13 module from the xylanase 10A of *Streptomyces lividans* (PDB ID 1KNL), with a RMSD of 1.5 Å over 124 residues and 17% sequence identity (Figure S6).

Overall, these results show that GH107 homolog sequences from members of the PVC superphylum present diverse domain architectures, including sequences only containing the putative GH107 domain, proteins containing novel domains for this family, and more complex domain architectures including regions previously identified in members of the GH107 family providing additional evidence of their close relationship with members of this family.

3.3. Characterization of a Fucanase from an Uncultured Planctomycete Bacterium

3.3.1. Recombinant Expression of OR07_113646

In order to assess if it presented fucoidan-degrading activity, the enzyme OR07_113646 was recombinantly expressed and characterized. The gene encoding for the OR07_113646 enzyme was amplified using fosmid DNA from the metagenomic library as template (without including the signal peptide region) and cloned into the pET28-TEV vector as a His-tag fusion. Soluble expression in *E. coli* BL21 (DE3) was achieved at low temperatures. The yield of the purified protein was 3.9 mg per L of 4xYT medium, at 12 °C. The enzyme OR07_113643 migrated as its predicted MW of approximately 42 kDa in an SDS-PAGE (Figure S7).

3.3.2. Enzyme Characterization

The activity of the OR07_113643 enzyme was evaluated using fucoidans purified from eight brown algae species from Patagonia, four of them including Ushuaia Bay (Tierra del Fuego, Argentina), in their geographic distribution (Table 1). The enzyme was only active against the fucoidan purified from *M. pyrifera*. After 25 min at 25 °C, C-PAGE analysis showed a similar pattern in the degradation of *M. pyrifera* fucoidan extracted from BL, GB, or ST (Figure 5A). The obtained profile, which showed decreasing amounts of HMWP and an increasing proportion of LMWP, is characteristic of endo-acting enzymes.

| Table 1. | Fucoidan | extracts | evaluated | in | this | work |
|----------|----------|----------|-----------|----|------|------|
| | | | | | | |

| Species | Order, Family | Activity | Reference | | |
|---------------------------|--------------------------------|----------|-----------|--|--|
| * Macrocystis pyrifera | Laminariales; Laminariaceae | yes | [75] | | |
| Undaria pinnatifida | Laminariales; Alariaceae | nd | [76] | | |
| * Adenocystis utricularis | Ectocarpales; Adenocystaceae | nd | [69] | | |
| * Scytosiphon lomentaria | Ectocarpales; Scytosiphonaceae | nd | [70] | | |
| * Colpomenia sinuosa | Ectocarpales; Scytosiphonaceae | nd | [72] | | |
| Eudesme virescens | Ectocarpales; Chordariaceae | nd | [72] | | |
| Myriogloea major | Ectocarpales; Chordariaceae | nd | [71] | | |
| Asperococcus ensiformis | Ectocarpales; Chordariaceae | nd | [72] | | |

^{*} Geographic distribution includes Ushuaia Bay (Tierra del Fuego, Argentina); nd, activity not detected in C-PAGE analyses after 25 min at 25 °C in 100 mM Tris-HCl (pH 7.5), 500 mM NaCl, 0.4% (w/v) fucoidan, and 1 μ M of the enzyme.

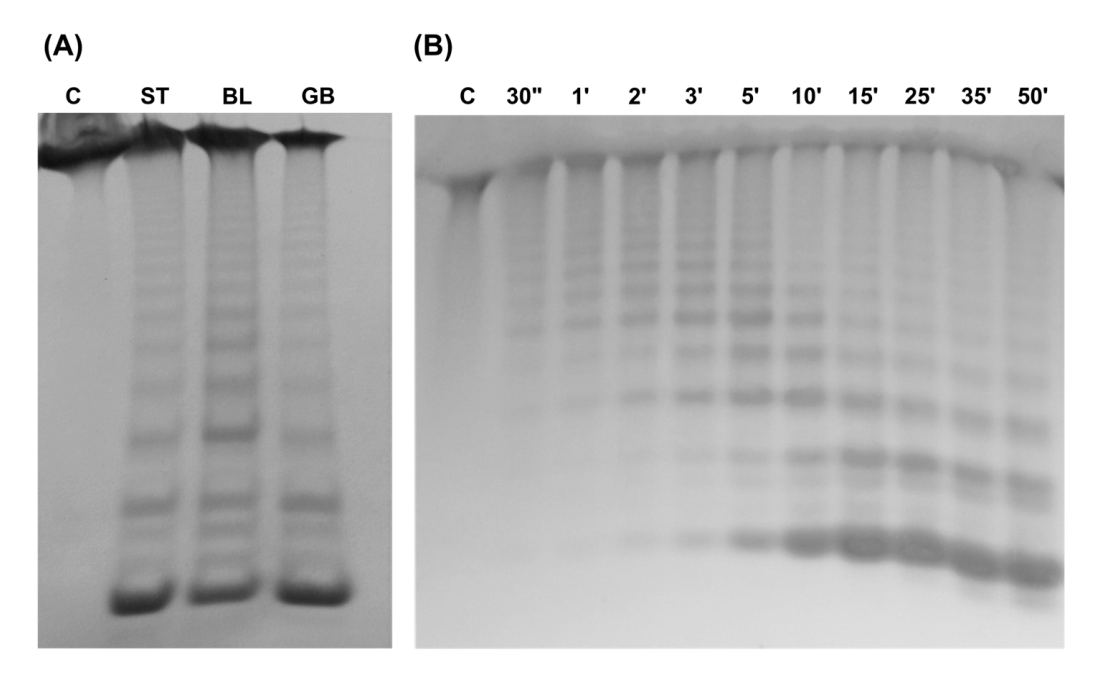


Figure 5. C-PAGE analysis of the hydrolysis of *M. pyrifera* fucoidan catalyzed by the enzyme OR07_113643. (**A**) Fucoidan extracts. C, control without enzyme; ST, fucoidan extracted from stipes; BL, fucoidan extracted from blades; GB, fucoidan extracted from gas bladders. (**B**) Incubation time. Hydrolysis of *M. pyrifera* fucoidan extracted from GB, at different incubation times at 25 °C. The reaction mixture contained 100 mM Tris-HCl (pH 7.5), 0.5 M NaCl, 0.4% (w/v) fucoidan, and 1 μM of the enzyme.

The hydrolysis of fucoidan reached a plateau after 15 min, and longer incubation times did not result in a higher proportion of LMWP (Figure 5B). The enzymatic activity was evaluated at NaCl concentrations between 9.5 mM and 1.24 M NaCl, with the activity only inhibited at the highest concentrations (Figure 6A). The enzyme was active at pH between 4.5 and 9.0, with an optimal range of 6.5 to 8.5 (Figure 6B). Optimal reaction temperatures were between 25 and 35 $^{\circ}$ C, although hydrolysis products were observed between 5 and 45 $^{\circ}$ C (Figure 6C).

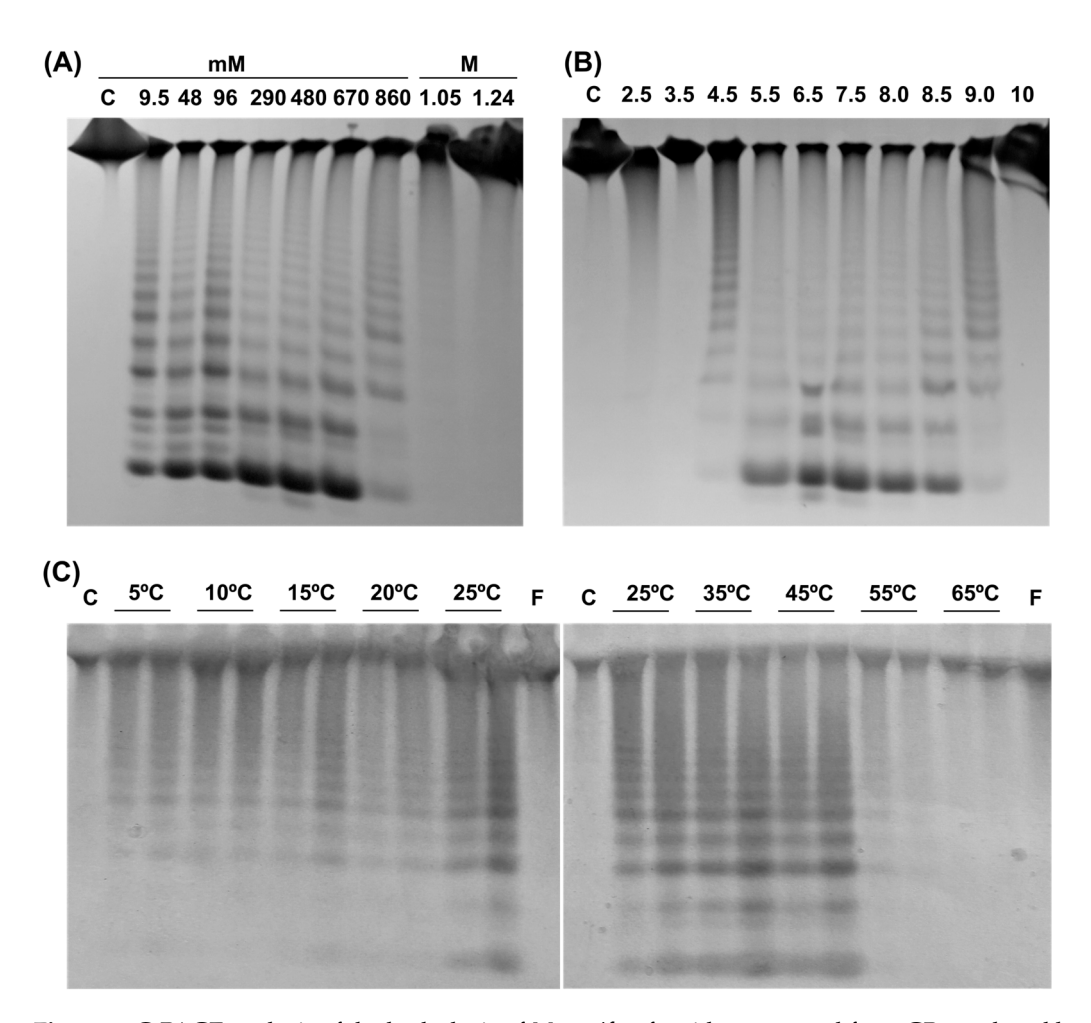


Figure 6. C-PAGE analysis of the hydrolysis of *M. pyrifera* fucoidan extracted from GB, catalyzed by the enzyme OR07_113643. (**A**) NaCl concentration. (**B**) pH. (**C**) Temperature, with incubations of 30 s and 1 min (left and right for each temperature, respectively). C, control of incubation without enzyme (left, 5 °C; right 65 °C); F, 150 μg fucoidan. Reaction conditions were 100 mM Tris-HCl (pH 7.5), 0.5 M NaCl, 0.4% (w/v) of fucoidan extracted from *M. pyrifera* GB, and 1 μM of enzyme at 25 °C unless otherwise indicated.

3.3.3. Composition and Structure of M. pyrifera Polysaccharide and Fuco-Oligosaccharides

The M. pyrifera fucoidan extracted from BL was used to characterize the polysaccharide and the LMWP generated after the hydrolysis by the fucanase from the uncultured planctomycete. The MW of M. pyrifera fucoidan used for the enzymatic reaction was estimated to be approximately 864 kDa (top of peak). The extract was fractionated by precipitation with cetrimide and redissolution with increasing concentrations of NaCl, to obtain four sulfated fractions (F1BL, F2BL, F3BL, and F4BL). The F4BL fraction was a highly sulfated polysaccharide containing mainly fucose and galactose in a 92:7 ratio (Table 2). The NMR analysis of this fraction suggested that the polysaccharide consists mainly of $(1\rightarrow 3)$ -linked fucopyranose residues within a 3-/4- alternating system, as the largest anomeric peak appears at 99.8/5.41 ppm [70,77].

| Extract/ | MW (kDa) * | Yield (%) | Carboh. (% anh.) | Uronate (% anh.) | Sulfate (% SO ₃ Na) | Neutral Monosaccharides (mol/100 mols) | | | | | | |
|----------|---------------|--------------|---------------------|---------------------|-----------------------------------|--|-----|-----|-----|-----|-----|-----|
| Fraction | | | | | | Rha | Fuc | Ara | Xyl | Man | Gal | Glc |
| BL | 864 | 6.0 | 50.2 | 5.7 | 29.4 | Tr. | 84 | 2 | 2 | 2 | 10 | Tr. |
| F4BL | 709.5 | 14.3 | 53.6 | Tr. | 41.4 | Tr. | 92 | Tr. | Tr. | Tr. | 7 | 1 |

46.7

F1-P2

1.82

11.6

Table 2. Analyses of the BL extract, F4BL fraction and F1-P2 of oligosaccharides from the degradation of BL extract of *M. pyrifera*.

100

nd

nd

nd

nd

nd

Nd

The enzymatic products were separated into HMWP and LMWP fractions by precipitation with ethanol. The LMWP fraction was further divided into subfractions F1-P2 and F2-P2, with different MW (Figure S8). The weights determined by GPC for the main peak were 1828 Da for F1-P2 and 655 Da for F2-P2 (top of the peak in both cases). Analysis of F1-P2 showed that fucose was the only monosaccharide component, with 46.7% sulfate (Table 2). The F1-P2 fraction was further investigated by NMR spectroscopy 2D (HSQC), showing the presence of α -L-Fucp oligosaccharides (Figure 7). A signal was observed at δ 91.1/5.53 ppm, which possibly corresponds to the reducing end residue α -(1 \rightarrow 3)-L-Fuc sulfated at O-2 [17,78,79]. However, the signal of the β -anomer was not observed, suggesting a large preference for this anomer upon mutarotation. Moreover, the signals at 99.6/5.37 ppm and 100.0/5.40 ppm were in agreement with those reported in the literature for \rightarrow 3)- α -L-Fucp2,4SO₃⁻ (1 \rightarrow and \rightarrow 3)- α -L-Fucp2SO₃⁻-(1 \rightarrow , respectively [18,23,27,79]. On the other hand, a signal was also observed at 95.5/5.41 ppm, which might correspond to 2-sulfated units linked at position 4 [25].

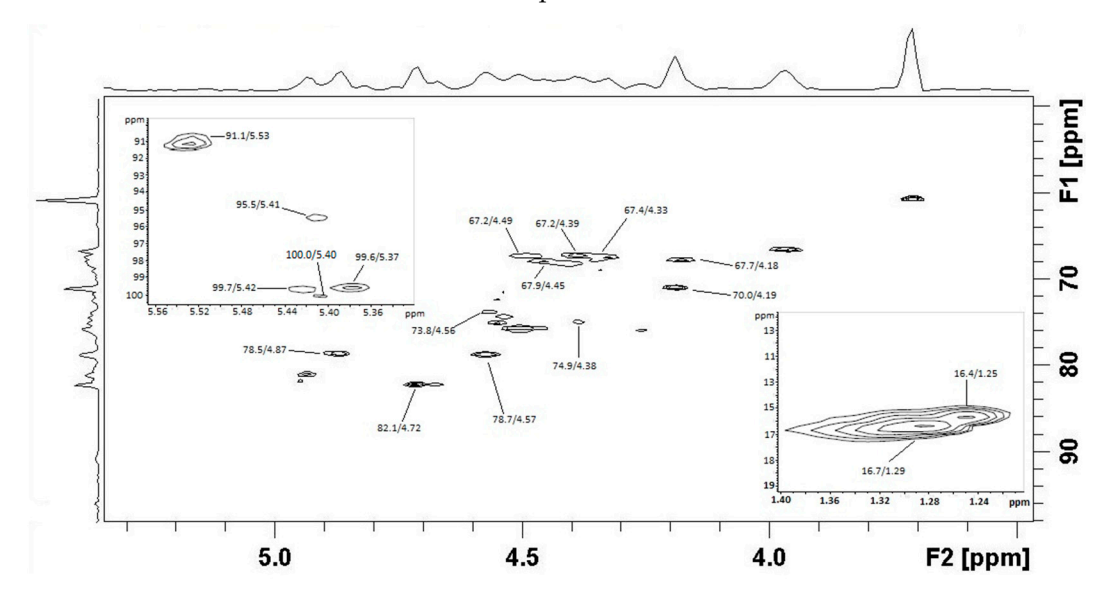


Figure 7. HSQC spectrum. F1-P2 fraction of the fuco-oligosaccharides generated by the hydrolysis of *M. pyrifera* fucoidan (BL) catalyzed by the enzyme OR07_113643.

The F1-P2 fraction was analyzed by ESI mass spectrometry (negative ion mode, Figure 8). The major peak suggested a structure of a fucose hexasaccharide substituted by one or two sulfate groups $[Fuc_6(SO_3Na)_{10}-3Na]^{3-}$. The ions at m/z 511.3925, 731.7430, and 934.0211 possibly correspond to $[Fuc_3(SO_3Na)_6-2Na]^{2-}$, $[Fuc_7(SO_3Na)_{12}-3Na]^{3-}$ and $[Fuc_6(SO_3Na)_{10}-2Na]^{2-}$ of 3, 7 and 6 monosaccharide units, respectively. Overall, these results indicate that the LMWPs produced by hydrolysis by the enzyme OR07_113643 present different lengths, containing a higher sulfate content than the substrate used in the reaction, suggesting a substrate specificity of the fucanase OR07_113643 for highly sulfated regions of the M. pyrifera fucoidan backbone.

^{*} Molecular weight (MW), as determined for the maximum value in the main peak of the GPC; Tr, traces (proportions lower than 0.5%); -, not determined; nd, not detected.

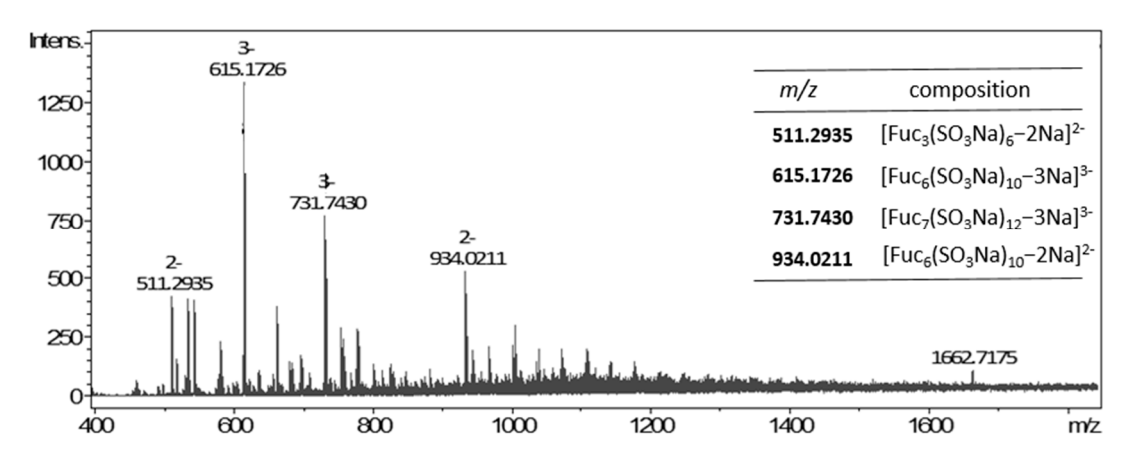


Figure 8. Negative ESI-MS spectra. F1-P2 fraction of the fuco-oligosaccharides fraction generated by the hydrolysis of *M. pyrifera* fucoidan catalyzed by the enzyme OR07_113643.

4. Discussion

Sequences homologous to members of the GH107 family assigned to the Planctomycetota phylum were identified in the two analyzed intertidal sediment metagenomes [35,36]. In particular, these sequences were abundant in the OR07 metagenomic dataset, which was generated by shotgun sequencing of fosmid DNA purified from a metagenomic library of intertidal sediments [36]. Conversely, the MM dataset was generated from a kelp-enriched community that presented a decreased abundance of members of Planctomycetota when compared to the sampled sediments [35], which could explain the lower abundance of putative GH107 sequences from Planctomycetota in this dataset. Sequences assigned to the Planctomycetota phylum were most closely related to GH107 homologs from MAGs and genomes of marine members of this phylum, suggesting that these organisms could play an important role in the assimilation of fucoidan in the marine environment. We explored the diversity of GH107 homolog sequences in genomes from organisms of the PVC superphylum, identifying sequences in members of the Planctomycetota (*Rhodopirellula* and *Novipirellula* spp.), Kiritimatiellota (*Pontiella* spp.), and Verrucomicrobiota (*Lentimonas* sp. CC4) phyla.

Lentimonas sp. CC4 (Verrucomicrobiota phylum) has been reported to present exceptional fucoidan degrading capabilities [4]. Sichert and collaborators [4] reported the presence of seven GH107 homolog sequences in the genome of this strain, among hundreds of putative enzymes related to the degradation of fucoidan from various species of brown algae. The authors detected the expression of three of the enzymes in Lentimonas sp. CC4, while no expression was observed in the other four putative genes. The search of GH107 homolog sequences in the genome of *Lentimonas* sp. CC4 in this work also resulted in the identification of seven putative enzymes with a complex domain architecture. The phylogenetic analysis showed a close relatedness of the seven GH107 homolog sequences identified in this organism with members of the GH107 family included in cluster C, identified in isolated bacteria from the Flavobacteriaceae family and from an uncultured bacterium [17,22-26]. These GH107 enzymes have been expressed and characterized, and it has been reported that they present endo- α -1,4-L-fucanase activity. Several sequences from this cluster contained a D1 domain followed by Ig-like R domain/s similar to MfFcnA [17,31]. The structure of the D1 and R1-R3 domains has been determined in the MfFcnA4 truncated enzyme by Vickers and collaborators [31]. Due to the absence of carbohydrate-binding sites, these authors suggested that the R1–R3 domains could function as a structural spacer separating the D1 catalytic module from the domains located at the Cterm end, often including a conserved all β -strand domain with unknown function [24,31]. Sequences WP_136081010 and WP_168433152 from Pontiella spp. contained a conserved all β-strand domain similar to the one of MfFcnA. The domain located after the conserved all β-strand domain, however, differed between the sequences from *Pontiella* spp. and MfFcnA.

On the other hand, one or two putative carbohydrate recognition domains with a fold similar to L-type lectins were identified in six of the sequences from *Lentimonas* sp. CC4, located in different positions of the deduced amino acid sequence, and in the fucanases Fp273 from an uncultured bacterium [22] and FWf2 and FWf3 from *W. fucanilytica* [24]. This domain presented a similar fold with a K⁺-dependent L-type Lectin that binds to mannose oligosaccharide chains from glycoproteins [80].

Other conserved domains commonly found in sequences of cluster C, both in members of the GH107 family and in sequences from organisms of the PVC superphylum, is the Concanavalin A-like lectin/glucanase domain superfamily (IPR013320), and the PF13385 (Laminin_G_3) domain. This domain, identified in four sequences from *Lentimonas* sp. CC4, is also present in Fda1 and Fda2 from Alteromonas sp. SN-1009 (cluster B1 of the phylogenetic tree) [24,31]. This domain has been found to function as a carbohydratebinding module in an arabinofuranosidase of the GH43 family from Ruminiclostridium josui, increasing the activity of this enzyme [81]. Another potential carbohydrate-binding domain was detected in sequence CAA6678285 from Lentimonas sp. CC4 as a ricin B lectin 2 domain (PF14200), an R-type lectin. This domain was annotated in the dbCAN2 server as CBM family 13, which is included in the ricin superfamily [82]. Members of this CBM family have been found to bind the polysaccharides xylan and alginate, as well as smaller molecules such as lactose and galactose [83–85]. A RicinB lectin domain (IPR000772) can also be detected in the sequence AXT50524 from *Aquimarina* sp. BL5, a GH107 member (cluster A). Overall, these results indicate that the similarity between members of the GH107 family and GH107 homolog sequences from members of the Planctomycetota, Verrucomicrobiota, and Kiritimatiellota phyla included in cluster C are not only limited to the D1 domain but also extends to other domains in these proteins.

The GH107 homolog sequences assigned to Planctomycetota from metagenomes of subantarctic sediments were most closely related to sequences identified in MAGs or genomes from members of the same phylum, including organisms associated with M. pyrifera blades from a kelp forest near Monterey Bay Aquarium, California [86]. This species has an extended geographic distribution including both hemispheres, and forests of this giant kelp can be found in cold-temperate coastal environments of Patagonia, including Ushuaia Bay [35,87]. All sequences from subcluster 1 contained an SLA1 homology domain 1 (SHD1, PF03983) at the N-term end, which has not been identified in members of the GH107 family. This domain has been described in yeast SLA1 proteins, participating in actin cytoskeleton assembly during endocytosis. The SHD1 domain presents an SH3-like fold with a hydrophobic binding site, which interacts with the NPFxD internalization signal of the transmembrane proteins [88]. In prokaryotic organisms, a subdomain with an SHD1-like structure (HSS subdomain) has been found in membrane coat-like proteins from organisms of the PVC superphylum, mainly from the Planctomycetota and Verrucomicrobiota phyla [74]. Many organisms from the PVC superphylum present a highly developed endomembrane system that results in a compartmentalized cell plan, with membrane-coat-like proteins located near the vesicles [89]. It has been suggested that the ability of Planctomycetes bacteria to engulf macromolecules for internal degradation could be linked to the endomembrane system [74].

We recombinantly expressed a putative enzyme identified in an intertidal sediment metagenome from a subantarctic environment. OR07_113643, most probably from an uncultured planctomycete. It belonged to cluster B2 (subcluster 1) of the phylogenetic tree that included no GH107 members. The goal was to assess if the expressed enzyme presented fucanase activity, as suggested by in silico structural analyses. The enzyme presented a high level of soluble expression in *E. coli*, and the MW of the purified protein suggested the presence of the SLA1 and D1 domains in the purified protein. The enzyme showed fucanase activity against sulfated polysaccharides purified from three different structures of the brown algae *M. pyrifera*. In kelp forests, algal fragments generated by physical and biological processes can be dislodged and buried locally in the sediments or transported long distances and eventually buried in offshore sediments [90]. Detritus of *M. pyrifera* and

other macroalgal species are often found beached in the Ushuaia Bay intertidal sediments, and the microbial community used to construct the OR07 metagenomic dataset might be often exposed to macroalgal polysaccharides [35,36,91]. Due to the structural diversity of fucoidans that can vary with the species, geographic location, season, among other factors [92], multiple enzymes with different specificities are expected to be present in the microbial community from this coastal environment.

The enzyme OR07_113643 showed activity against fucoidans after short incubation times, and in a wide range of temperatures, pH, and NaCl concentrations. The enzyme presented a high enzymatic activity without Ca²⁺ addition, although the effect of chelation was not investigated. Several fucanases require Ca²⁺ or the activity was activated by Ca²⁺ or other cations [16,23,25,27]. This is the case of the D1 domain of the Fhf2 enzyme from Formosa haliotis, where two Ca²⁺ binding sites were predicted [27]. The fucanase enzyme characterized in this work presented the highest activity at NaCl concentrations close to the salinity values measured in Ushuaia Bay (15 in spring and 32 in winter [93]), which is lower than the average seawater salinity (35, ~0.6 M with NaCl as the main component [94]). Other fucanase enzymes showed optimal NaCl concentrations below seawater salinity values, e.g., Fhf2 Δ 484 from the marine flavobacterium F. haliotis [27], the fucanases purified from Alteromonas sp. SN-1009 [29], and Mef1 from A. eckloniae [32]. However, the optimal NaCl concentrations for enzymatic activity has not been reported for the majority of the characterized fucanase enzymes. In agreement with the low activity at high NaCl concentrations, the predicted surface electrostatic potential of OR07_113643 showed few negative regions, a characteristic that was also found in the models of other sequences from subclusters 1 and 2 and in Mef1, which is completely inactivated at 500 mM NaCl [32]. High salt concentrations affect the native structure and function of the protein by reducing its hydration shell. An increase in acidic residues at the protein surface, resulting in a low surface electrostatic potential, has been related to adaptations to high salinities [95].

The diversity and specificities of fucoidan-degrading enzymes are just starting to emerge [18,19,32,96,97]. The OR07_113643 fucanase enzyme catalyzed the cleavage of internal glycosidic linkages of fucoidans from the widely distributed giant kelp M. pyrifera. Other fucanase enzymes that showed specificity for this substrate include P5AFcnA from Psychromonas sp. SW5A, P19DFcnA from Psychromonas sp. SW19D, and Swfcn2 from Flavobacterium sp. SW [31,98], although the evaluation of this substrate has not been reported for most fucanases. The study of the enzymatic depolymerization of M. pyrifera fucoidan is hindered by its complex and poorly understood structure, as is the case with the fucoidans of many brown algae species [16,99]. In this work, we first analyzed the composition of monosaccharides of the fucoidans extracted from M. pyrifera of Patagonia, which showed fucose and galactose as the main components. This result was in agreement with the composition reported by Lorbeer et al. [100], Zhang et al. [101], and Sichert et al. [99]. On the other hand, Zou and collaborators [75] reported a composition with a high proportion of other monosaccharides such as mannose and xylose. The composition may vary according to the purification level of the sulfated polysaccharides, producing inconsistencies in the results that are difficult to differentiate from natural compositional variations [92,99].

The NMR analysis of a highly purified fraction of the fucoidan extracted from M. pyrifera indicated that the fucose units presented mostly α - $(1\rightarrow 3)$ -glycosidic linkages, within an alternating system of α - $(1\rightarrow 3)$ and α - $(1\rightarrow 4)$ bonds. This structure is similar to fucoidans of species of the order Fucales [22]. Other fucoidans evaluated in this study present different structures. S. lomentaria contains a highly sulfated fucoidan with 3-linked α -L-fucopyranosyl units, also containing 6-linked galactose and 2-linked mannose [70]. A. utricularis, on the other hand, contains both a galactofucan with 3-linked α -L-fucopyranosyl units and an uronofucoidan [69]. U. pinnatifida contains a galactofucan with a fucosegalactose backbone linked by 1,3 glycosidic bonds [102]. No structural information is available for the remaining sulfated polysaccharides evaluated in this work. Among these sulfated polysaccharides with various structures, enzymatic activity was only detected in

OR07_113643 for *M. pyrifera* fucoidan, in the assayed conditions. The microbial community from Ushuaia Bay sediments are probably exposed to the fucoidans of four of these species, *M. pyrifera*, *A. utricularis*, *S. lomentaria*, and *C. sinuosa* (with unknown structure), as these species are present in subantarctic environments of Southern Patagonia [103].

The enzymatic hydrolysis of M. pyrifera fucoidan by the fucanase OR07_113643 resulted in the generation of oligosaccharides with different degrees of polymerization, mainly tri-, hexa-, and heptasaccharides, and polysaccharides with different MW, producing the typical laddering pattern of endo-acting hydrolases in the C-PAGE analysis [31]. The oligosaccharides presented a high degree of sulfation, which has previously been related to high bioactivity [27]. The structural analysis of the purified LMW enzymatic products showed that the fuco-oligosaccharides present a backbone with α -(1 \rightarrow 4)-linked L-fucose residues with monosulfated (C2 position) and disulfated (C2 and C4 positions) units. This result was consistent with the structural analysis of the purified fucoidan from this species. The absence of enzymatic activity in the case of 3-linked S. lomentaria fucoidan suggest a specificity for α -(1 \rightarrow 4)-bonds; although previous works indicated that the specificity of the fucanases depends not only on the type of glycosidic bond present in the backbone of the polysaccharide but also on specific sulfation and ramification patterns [19,31]. Therefore, the specific glycosidic linkage recognized by the enzyme needs to be further evaluated due to the complexity of the structure of M. pyrifera fucoidan.

5. Conclusions

This study expands the knowledge of the fucoidan-degrading potential of organisms from the Planctomycetota, Verrucomicrobiota, and Kiritimatiellota phyla, with the identification of two groups of sequences from members of these phyla, with different levels of phylogenetic relationships with enzymes of the GH107 family. The fucanase activity was confirmed in an enzyme from a cluster of novel sequences with modeled structural characteristics highly conserved in the catalytic modules of the GH107 family. Due to its high level of recombinant expression and enzymatic activity in a wide range of conditions, this enzyme could be of interest for the biocatalytic production of fuco-oligosaccharides from *M. pyrifera*.

Supplementary Materials: The following supporting information can be downloaded at: https://www. mdpi.com/article/10.3390/jmse12010181/s1, Table S1: dbCAN2 and CUPP annotations of OR07 and MM metagenomic datasets; Table S2: Closest sequences of the NCBI NR database identified using the BLASTp algorithm, and included in the SSN (Figure 1); Table S3: Sequences included in the clusters and subclusters of the SSN (Figure 1); Table S4: Sequences from genomes/MAGs of members of the PVC superphylum, and metagenomic sequences assigned to the Planctomycetota phylum; Table S5: Domain architecture of sequences from members of the PVC superphylum; Figure S1: Alignment of sequences identified in members of the PVC superphylum; Figure S2: Surface electrostatic potential and overall structure of models from putative GH107 sequences and experimentally determined structures; Figure S3: Calcium binding sites in the D1 domains; Figure S4: SLA1 homology domain 1; Figure S5: Comparison of the N-terminal region of sequence CAA6678994 from Lentimonas sp. CC4 and structure 2A6Z; Figure S6: Comparison of the C-terminal region of sequence CAA6678285 from Lentimonas sp. CC4 and structure 1KNL; Figure S7: SDS-PAGE analysis of the recombinant expression of the fucanase OR07_113643; Figure S8: Purification of LMW products of the hydrolysis of M. pyrifera fucoidan by the enzyme OR07_113643 in Bio-Gel P-2 column; Figure S9: Quality indicators of the models used in this work; ANNEX: Sequences identified and/or analyzed in this study.

Author Contributions: Conceptualization, H.M.D.; methodology, J.A.G., N.M.A.P., Y.D. and H.M.D.; validation, J.A.G., N.M.A.P. and H.M.D.; formal analysis, J.A.G., N.M.A.P., C.A.S., M.L. and H.M.D.; investigation, J.A.G., N.M.A.P., M.L., Y.D. and H.M.D.; data curation, M.L. and H.M.D.; writing—original draft preparation, J.A.G. and H.M.D.; writing—review and editing, J.A.G., N.M.A.P., M.L., Y.D., C.A.S. and H.M.D.; visualization, J.A.G., N.M.A.P. and H.M.D.; supervision, H.M.D. and N.M.A.P.; funding acquisition, H.M.D., C.A.S. and N.M.A.P. All authors have read and agreed to the published version of the manuscript.

Funding: This work was supported by grants from the University of Buenos Aires (20020170100255BA), National Research Council of Argentina-CONICET (PIP 298/14 and P-UE 22920160100068CO), ANPCyT-Argentina (PICT 2017-1675 and PICT 2016-2101) and "Programa Investigación, Desarrollo e Innovación en Ciencias del Mar de la Iniciativa Pampa Azul" (C-20).

Institutional Review Board Statement: Not applicable.

Informed Consent Statement: Not applicable.

Data Availability Statement: Metagenomic sequences analyzed in this work have been deposited in the NCBI database under Accession numbers: MM (OP559563, OP559567, OP559592, OP559602, OP559612, OP559618, OP559620, OP559626, OP559658, OP559666, OP559675, OP559678, OP559687, OP559696, OP559700, OP559704, OP559706, OP559710, OP559726, OP559779, OP559780, OP559781, OP559808, OP559809, OP559816, OP559819, OP559833, OP559835, OP559845, OP559879, OP559907, OP559908, OP559910, OP559924, OP559926, OP559936, OP559938, OP559950, OP559960, OP559968, OP559981, OP559982, OP559987, OP559992, OP559993, OR545406); OR07 (OR545400–OR545405, PP035745–PP035748).

Acknowledgments: J.A.G. is a doctoral fellows of the Argentinean National Research Council (CONICET). N.M.A.P., Y.D., M.L., C.A.S. and H.M.D. are staff members of CONICET. We would like to thank Ezequiel Latour and Fernando Dellatorre for kindly providing the fucoidans from *M. major*, *E. virescens*, *C. sinuosa*, and *A. ensiformis* to test as substrates for the fucanase, and María Paula Raffo for her assistance with macroalgae taxonomy. We are thankful to Diego Navarro for his help with GPC determinations.

Conflicts of Interest: The authors declare no conflicts of interest. The funders had no role in the design of the study; in the collection, analyses, or interpretation of data; in the writing of the manuscript; or in the decision to publish the results.

References

- Van Niftrik, L.; Devos, D.P. Planctomycetes-Verrucomicrobia-Chlamydiae bacterial superphylum: New model organisms for evolutionary cell biology. Front. Microbiol. 2017, 8, 1458.
- 2. Vitorino, I.R.; Lage, O.M. The Planctomycetia: An overview of the currently largest class within the phylum Planctomycetes. *Antonie Van Leeuwenhoek* **2022**, *115*, 169–201. [CrossRef]
- 3. Zhang, T.; Zheng, R.; Liu, R.; Li, R.; Sun, C. Cultivation and functional characterization of a deep-sea Lentisphaerae representative reveals its unique physiology and ecology. *Front. Mar. Sci.* **2022**, *9*, 458. [CrossRef]
- 4. Sichert, A.; Corzett, C.H.; Schechter, M.S.; Unfried, F.; Markert, S.; Becher, D.; Fernandez-Guerra, A.; Liebeke, M.; Schweder, T.; Polz, M.F. Verrucomicrobia use hundreds of enzymes to digest the algal polysaccharide fucoidan. *Nat. Microbiol.* **2020**, 5, 1026–1039. [CrossRef]
- 5. Dharamshi, J.E.; Tamarit, D.; Eme, L.; Stairs, C.W.; Martijn, J.; Homa, F.; Jørgensen, S.L.; Spang, A.; Ettema, T.J. Marine sediments illuminate Chlamydiae diversity and evolution. *Curr. Biol.* **2020**, *30*, 1032–1048. [CrossRef]
- 6. Freitas, S.; Hatosy, S.; Fuhrman, J.A.; Huse, S.M.; Mark Welch, D.B.; Sogin, M.L.; Martiny, A.C. Global distribution and diversity of marine Verrucomicrobia. *ISME J.* **2012**, *6*, 1499–1505. [CrossRef]
- 7. Wiegand, S.; Jogler, M.; Jogler, C. On the maverick Planctomycetes. FEMS Microbiol. Rev. 2018, 42, 739–760.
- 8. Bondoso, J.; Godoy-Vitorino, F.; Balague, V.; Gasol, J.M.; Harder, J.; Lage, O.M. Epiphytic Planctomycetes communities associated with three main groups of macroalgae. *FEMS Microbiol. Ecol.* **2017**, *93*, fiw255. [CrossRef]
- Lage, O.M.; Bondoso, J. Planctomycetes and macroalgae, a striking association. Front. Microbiol. 2014, 5, 267. [CrossRef]
- 10. Vollmers, J.; Frentrup, M.; Rast, P.; Jogler, C.; Kaster, A.-K. Untangling genomes of novel planctomycetal and verrucomicrobial species from Monterey Bay kelp forest metagenomes by refined binning. *Front. Microbiol.* **2017**, *8*, 472. [CrossRef]
- 11. Lozada, M.; Diéguez, M.C.; García, P.E.; Bigatti, G.; Livore, J.P.; Giarratano, E.; Gil, M.N.; Dionisi, H.M. *Undaria pinnatifida* exudates trigger shifts in seawater chemistry and microbial communities from Atlantic Patagonian coasts. *Biol. Invasions* **2021**, 23, 1781–1801. [CrossRef]
- 12. Reintjes, G.; Arnosti, C.; Fuchs, B.; Amann, R. Selfish, sharing and scavenging bacteria in the Atlantic Ocean: A biogeographical study of bacterial substrate utilisation. *ISME J.* **2019**, *13*, 1119–1132. [CrossRef]
- 13. Van Vliet, D.M.; Palakawong Na Ayudthaya, S.; Diop, S.; Villanueva, L.; Stams, A.J.; Sánchez-Andrea, I. Anaerobic degradation of sulfated polysaccharides by two novel Kiritimatiellales strains isolated from Black Sea sediment. *Front. Microbiol.* **2019**, *10*, 253. [CrossRef] [PubMed]
- 14. Martins, A.; Alves, C.; Silva, J.; Pinteus, S.; Gaspar, H.; Pedrosa, R. Sulfated polysaccharides from macroalgae—A simple roadmap for chemical characterization. *Polymers* **2023**, *15*, 399. [CrossRef] [PubMed]
- Haggag, Y.A.; Abd Elrahman, A.A.; Ulber, R.; Zayed, A. Fucoidan in pharmaceutical formulations: A comprehensive review for smart drug delivery systems. Mar. Drugs 2023, 21, 112. [CrossRef]

16. Kusaykin, M.I.; Silchenko, A.S.; Zakharenko, A.M.; Zvyagintseva, T.N. Fucoidanases. *Glycobiology* **2016**, 26, 3–12. [CrossRef] [PubMed]

- 17. Colin, S.; Deniaud, E.; Jam, M.; Descamps, V.; Chevolot, Y.; Kervarec, N.; Yvin, J.-C.; Barbeyron, T.; Michel, G.; Kloareg, B. Cloning and biochemical characterization of the fucanase FcnA: Definition of a novel glycoside hydrolase family specific for sulfated fucans. *Glycobiology* **2006**, *16*, 1021–1032. [CrossRef] [PubMed]
- 18. Shen, J.; Chang, Y.; Zhang, Y.; Mei, X.; Xue, C. Discovery and characterization of an endo-1, 3-fucanase from marine bacterium *Wenyingzhuangia fucanilytica*: A novel glycoside hydrolase family. *Front. Microbiol.* **2020**, *11*, 1674. [CrossRef]
- 19. Liu, G.; Shen, J.; Chang, Y.; Mei, X.; Chen, G.; Zhang, Y.; Xue, C. Characterization of an endo-1, 3-fucanase from marine bacterium *Wenyingzhuangia aestuarii*: The first member of a novel glycoside hydrolase family GH174. *Carbohydr. Polym.* **2023**, 306, 120591. [CrossRef]
- 20. Shen, J.; Zheng, L.; Zhang, Y.; Chen, G.; Mei, X.; Chang, Y.; Xue, C. Discovery of a catalytic domain defines a new glycoside hydrolase family containing endo-1,3-fucanase. *Carbohydr. Polym.* **2024**, 323, 121442.
- 21. Drula, E.; Garron, M.-L.; Dogan, S.; Lombard, V.; Henrissat, B.; Terrapon, N. The carbohydrate-active enzyme database: Functions and literature. *Nucleic Acids Res.* **2022**, *50*, D571–D577. [CrossRef]
- 22. Schultz-Johansen, M.; Cueff, M.; Hardouin, K.; Jam, M.; Larocque, R.; Glaring, M.A.; Hervé, C.; Czjzek, M.; Stougaard, P. Discovery and screening of novel metagenome-derived GH 107 enzymes targeting sulfated fucans from brown algae. *FEBS J.* **2018**, 285, 4281–4295.
- Silchenko, A.S.; Ustyuzhanina, N.E.; Kusaykin, M.I.; Krylov, V.B.; Shashkov, A.S.; Dmitrenok, A.S.; Usoltseva, R.V.; Zueva, A.O.; Nifantiev, N.E.; Zvyagintseva, T.N. Expression and biochemical characterization and substrate specificity of the fucoidanase from Formosa algae. Glycobiology 2017, 27, 254–263.
- Zueva, A.; Silchenko, A.; Rasin, A.; Kusaykin, M.; Usoltseva, R.; Kalinovsky, A.; Kurilenko, V.; Zvyagintseva, T.; Thinh, P.; Ermakova, S. Expression and biochemical characterization of two recombinant fucoidanases from the marine bacterium Wenyingzhuangia fucanilytica CZ1127T. Int. J. Biol. Macromol. 2020, 164, 3025–3037. [PubMed]
- 25. Vuillemin, M.; Silchenko, A.S.; Cao, H.T.T.; Kokoulin, M.S.; Trang, V.T.D.; Holck, J.; Ermakova, S.P.; Meyer, A.S.; Mikkelsen, M.D. Functional characterization of a new GH107 endo-α-(1,4)-fucoidanase from the marine bacterium *Formosa haliotis*. *Mar. Drugs* **2020**, *18*, 562. [CrossRef] [PubMed]
- 26. Qiu, Y.; Jiang, H.; Dong, Y.; Wang, Y.; Hamouda, H.I.; Balah, M.A.; Mao, X. Expression and biochemical characterization of a novel fucoidanase from *Flavobacterium algicola* with the principal product of fucoidan-derived disaccharide. *Foods* **2022**, *11*, 1025. [PubMed]
- 27. Trang, V.T.D.; Mikkelsen, M.D.; Vuillemin, M.; Meier, S.; Cao, H.T.T.; Muschiol, J.; Perna, V.; Nguyen, T.T.; Tran, V.H.N.; Holck, J. The endo-α (1,4) specific fucoidanase Fhf2 from *Formosa haliotis* releases highly sulfated fucoidan oligosaccharides. *Front. Plant Sci.* **2022**, *13*, 823668. [CrossRef]
- 28. Tran, V.H.N.; Nguyen, T.T.; Meier, S.; Holck, J.; Cao, H.T.T.; Van, T.T.T.; Meyer, A.S.; Mikkelsen, M.D. The endo-α (1,3)-fucoidanase Mef2 releases uniquely branched oligosaccharides from *Saccharina latissima* fucoidans. *Mar. Drugs* **2022**, *20*, 305.
- 29. Sakai, T.; Kawai, T.; Kato, I. Isolation and characterization of a fucoidan-degrading marine bacterial strain and its fucoidanase. *Mar. Biotechnol.* **2004**, *6*, 335–346. [CrossRef]
- 30. Zhu, C.; Liu, Z.; Ren, L.; Jiao, S.; Zhang, X.; Wang, Q.; Li, Z.; Du, Y.; Li, J.-J. Overexpression and biochemical characterization of a truncated endo-α (1→3)-fucoidanase from *Alteromonas* sp. SN-1009. *Food Chem.* **2021**, *353*, 129460. [CrossRef]
- 31. Vickers, C.; Liu, F.; Abe, K.; Salama-Alber, O.; Jenkins, M.; Springate, C.M.; Burke, J.E.; Withers, S.G.; Boraston, A.B. Endo-fucoidan hydrolases from glycoside hydrolase family 107 (GH107) display structural and mechanistic similarities to α-L-fucosidases from GH29. *J. Biol. Chem.* **2018**, 293, 18296–18308. [CrossRef] [PubMed]
- 32. Tran, V.H.N.; Nguyen, T.T.; Meier, S.; Holck, J.; Cao, H.T.T.; Van, T.T.T.; Meyer, A.S.; Mikkelsen, M.D. Structural and functional characterization of the novel endo-α(1,4)-fucoidanase Mef1 from the marine bacterium *Muricauda eckloniae*. *Acta Crystallogr. D Struct. Biol.* **2023**, *79*, 1026–1043.
- 33. Sakai, T.; Ishizuka, K.; Kato, I. Isolation and characterization of a fucoidan-degrading marine bacterium. *Mar. Biotechnol.* **2003**, 5, 409–416. [CrossRef] [PubMed]
- 34. Ohshiro, T.; Harada, N.; Kobayashi, Y.; Miki, Y.; Kawamoto, H. Microbial fucoidan degradation by *Luteolibacter algae* H18 with deacetylation. *Biosci. Biotechnol. Biochem.* **2012**, 76, 620–623. [CrossRef]
- 35. Lozada, M.; Diéguez, M.C.; García, P.E.; Dionisi, H.M. Microbial communities associated with kelp detritus in temperate and subantarctic intertidal sediments. *Sci. Total Environ.* **2023**, *857*, 159392. [CrossRef]
- 36. Dionisi, H.M.; Lozada, M.; Campos, E. Diversity of GH51 α-L-arabinofuranosidase homolog sequences from subantarctic intertidal sediments. *Biologia* **2023**, *78*, 1899–1918.
- 37. Zhu, W.; Lomsadze, A.; Borodovsky, M. *Ab initio* gene identification in metagenomic sequences. *Nucleic Acids Res.* **2010**, *38*, e132. [CrossRef]
- 38. Tamames, J.; Puente-Sánchez, F. SqueezeMeta, A Highly Portable, Fully Automatic Metagenomic Analysis Pipeline. *Front. Microbiol.* **2019**, *9*, 3349.
- 39. Li, D.; Liu, C.-M.; Luo, R.; Sadakane, K.; Lam, T.-W. MEGAHIT: An ultra-fast single-node solution for large and complex metagenomics assembly via succinct de Bruijn graph. *Bioinformatics* **2015**, *31*, 1674–1676.

40. Hyatt, D.; Chen, G.-L.; LoCascio, P.F.; Land, M.L.; Larimer, F.W.; Hauser, L.J. Prodigal: Prokaryotic gene recognition and translation initiation site identification. *BMC Bioinform.* **2010**, *11*, 119.

- 41. Commendatore, M.G.; Nievas, M.L.; Amin, O.; Esteves, J.L. Sources and distribution of aliphatic and polyaromatic hydrocarbons in coastal sediments from the Ushuaia Bay (Tierra del Fuego, Patagonia, Argentina). *Mar. Environ. Res.* **2012**, 74, 20–31. [PubMed]
- 42. Gil, M.N.; Torres, A.I.; Amin, O.; Esteves, J.L. Assessment of recent sediment influence in an urban polluted subantarctic coastal ecosystem. Beagle Channel (Southern Argentina). *Mar. Pollut. Bull.* **2011**, *62*, 201–207. [CrossRef] [PubMed]
- 43. Zhang, H.; Yohe, T.; Huang, L.; Entwistle, S.; Wu, P.; Yang, Z.; Busk, P.K.; Xu, Y.; Yin, Y. dbCAN2: A meta server for automated carbohydrate-active enzyme annotation. *Nucleic Acids Res.* **2018**, *46*, W95–W101. [PubMed]
- 44. Barrett, K.; Hunt, C.J.; Lange, L.; Meyer, A.S. Conserved unique peptide patterns (CUPP) online platform: Peptide-based functional annotation of carbohydrate active enzymes. *Nucleic Acids Res.* **2020**, *48*, W110–W115. [PubMed]
- 45. Pruitt, K.D.; Tatusova, T.; Maglott, D.R. NCBI reference sequences (RefSeq): A curated non-redundant sequence database of genomes, transcripts and proteins. *Nucleic Acids Res.* **2007**, 35, D61–D65. [CrossRef]
- 46. Chen, I.-M.A.; Chu, K.; Palaniappan, K.; Ratner, A.; Huang, J.; Huntemann, M.; Hajek, P.; Ritter, S.; Varghese, N.; Seshadri, R. The IMG/M data management and analysis system v. 6.0: New tools and advanced capabilities. *Nucleic Acids Res.* **2021**, 49, D751–D763.
- 47. Johnson, M.; Zaretskaya, I.; Raytselis, Y.; Merezhuk, Y.; McGinnis, S.; Madden, T.L. NCBI BLAST: A better web interface. *Nucleic Acids Res.* **2008**, *36*, W5–W9.
- 48. Eddy, S.R. Accelerated profile HMM searches. PLoS Comput. Biol. 2011, 7, e1002195. [CrossRef]
- 49. Huson, D.H.; Beier, S.; Flade, I.; Górska, A.; El-Hadidi, M.; Mitra, S.; Ruscheweyh, H.-J.; Tappu, R. MEGAN community edition-interactive exploration and analysis of large-scale microbiome sequencing data. *PLoS Comput. Biol.* **2016**, *12*, e1004957. [CrossRef]
- 50. Schoch, C.L.; Ciufo, S.; Domrachev, M.; Hotton, C.L.; Kannan, S.; Khovanskaya, R.; Leipe, D.; Mcveigh, R.; O'Neill, K.; Robbertse, B. NCBI Taxonomy: A comprehensive update on curation, resources and tools. *Database* **2020**, 2020, baaa062. [CrossRef]
- 51. Oberg, N.; Zallot, R.; Gerlt, J.A. EFI-EST, EFI-GNT, and EFI-CGFP: Enzyme Function Initiative (EFI) web resource for genomic enzymology tools. *J. Molec. Biol.* **2023**, *435*, 168018.
- 52. Shannon, P.; Markiel, A.; Ozier, O.; Baliga, N.S.; Wang, J.T.; Ramage, D.; Amin, N.; Schwikowski, B.; Ideker, T. Cytoscape: A software environment for integrated models of biomolecular interaction networks. *Genome Res.* 2003, 13, 2498–2504. [CrossRef] [PubMed]
- 53. Larkin, M.A.; Blackshields, G.; Brown, N.P.; Chenna, R.; McGettigan, P.A.; McWilliam, H.; Valentin, F.; Wallace, I.M.; Wilm, A.; Lopez, R. Clustal W and Clustal X version 2.0. *Bioinformatics* **2007**, *23*, 2947–2948.
- 54. Waterhouse, A.M.; Procter, J.B.; Martin, D.M.; Clamp, M.; Barton, G.J. Jalview Version 2—A multiple sequence alignment editor and analysis workbench. *Bioinformatics* **2009**, *25*, 1189–1191. [PubMed]
- 55. Tamura, K.; Stecher, G.; Kumar, S. MEGA11: Molecular Evolutionary Genetics Analysis Version 11. *Mol. Biol. Evol.* **2021**, *38*, 3022–3027. [CrossRef] [PubMed]
- 56. Teufel, F.; Almagro Armenteros, J.J.; Johansen, A.R.; Gíslason, M.H.; Pihl, S.I.; Tsirigos, K.D.; Winther, O.; Brunak, S.; von Heijne, G.; Nielsen, H. SignalP 6.0 predicts all five types of signal peptides using protein language models. *Nat. Biotechnol.* **2022**, 40, 1023–1025. [CrossRef]
- 57. Hallgren, J.; Tsirigos, K.D.; Pedersen, M.D.; Almagro Armenteros, J.J.; Marcatili, P.; Nielsen, H.; Krogh, A.; Winther, O. DeepTMHMM predicts alpha and beta transmembrane proteins using deep neural networks. *BioRxiv* **2022**, preprint. [CrossRef]
- 58. Blum, M.; Chang, H.-Y.; Chuguransky, S.; Grego, T.; Kandasaamy, S.; Mitchell, A.; Nuka, G.; Paysan-Lafosse, T.; Qureshi, M.; Raj, S. The InterPro protein families and domains database: 20 years on. *Nucleic Acids Res.* **2021**, 49, D344–D354. [CrossRef]
- 59. Marchler-Bauer, A.; Derbyshire, M.K.; Gonzales, N.R.; Lu, S.; Chitsaz, F.; Geer, L.Y.; Geer, R.C.; He, J.; Gwadz, M.; Hurwitz, D.I. CDD: NCBI's conserved domain database. *Nucleic Acids Res.* **2015**, *43*, D222–D226.
- 60. Mirdita, M.; Schütze, K.; Moriwaki, Y.; Heo, L.; Ovchinnikov, S.; Steinegger, M. ColabFold: Making protein folding accessible to all. *Nat. Methods* **2022**, *19*, 679–682.
- 61. Pettersen, E.F.; Goddard, T.D.; Huang, C.C.; Meng, E.C.; Couch, G.S.; Croll, T.I.; Morris, J.H.; Ferrin, T.E. UCSF ChimeraX: Structure visualization for researchers, educators, and developers. *Protein Sci.* **2021**, *30*, 70–82. [PubMed]
- 62. Holm, L. Dali server: Structural unification of protein families. Nucleic Acids Res. 2022, 50, W210-W215. [CrossRef] [PubMed]
- 63. Yariv, B.; Yariv, E.; Kessel, A.; Masrati, G.; Chorin, A.B.; Martz, E.; Mayrose, I.; Pupko, T.; Ben-Tal, N. Using evolutionary data to make sense of macromolecules with a "face-lifted" ConSurf. *Protein Sci.* **2023**, *32*, e4582.
- 64. Laemmli, U.K. Cleavage of structural proteins during the assembly of the head of bacteriophage T4. *Nature* **1970**, 227, 680–685. [CrossRef] [PubMed]
- 65. Bradford, M.M. A rapid and sensitive method for the quantitation of microgram quantities of protein utilizing the principle of protein-dye binding. *Anal. Biochem.* **1976**, 72, 248–254. [CrossRef] [PubMed]
- 66. Dubois, M.; Gilles, K.; Hamilton, J.; Rebers, P.; Smith, F. A colorimetric method for the determination of sugars. *Nature* **1951**, 168, 167. [CrossRef]
- 67. Filisetti-Cozzi, T.M.; Carpita, N.C. Measurement of uronic acids without interference from neutral sugars. *Anal. Biochem.* **1991**, 197, 157–162.

J. Mar. Sci. Eng. **2024**, 12, 181 25 of 26

68. Dodgson, K.; Price, R. A note on the determination of the ester sulphate content of sulphated polysaccharides. *Biochem. J.* **1962**, 84, 106. [CrossRef]

- 69. Ponce, N.M.; Pujol, C.A.; Damonte, E.B.; Flores, M.a.L.; Stortz, C.A. Fucoidans from the brown seaweed *Adenocystis utricularis*: Extraction methods, antiviral activity and structural studies. *Carbohydr. Res.* **2003**, *338*, 153–165. [CrossRef]
- 70. Ponce, N.M.; Flores, M.L.; Pujol, C.A.; Becerra, M.B.; Navarro, D.A.; Córdoba, O.; Damonte, E.B.; Stortz, C.A. Fucoidans from the phaeophyta *Scytosiphon lomentaria*: Chemical analysis and antiviral activity of the galactofucan component. *Carbohydr. Res.* **2019**, 478. 18–24.
- 71. Conesa, A.L.; Dellatorre, F.G.; Latour, E.; Ponce, N.M.A.; Stortz, C.A.; Scolaro, L.A.; Álvarez, V.A.; Lassalle, V.L. Potential of Fucoidan From *Myriogloea Major* Asensi as Antiviral Against Herpes Simplex Type 1 and 2 and Bovine Coronavirus. *Res. Sq.* **2023**, preprint. [CrossRef]
- 72. Latour, E.; Dellatorre, F.G.; Ponce, N.M.A. Cuantificación y caracterización de fucoidanos de distintas algas pardas del Golfo Nuevo, Chubut, Argentina. *Actas De Jorn. Y Even. Académicos De UTN* **2022**, *15*, 1–6. [CrossRef]
- 73. Atkinson, H.J.; Morris, J.H.; Ferrin, T.E.; Babbitt, P.C. Using sequence similarity networks for visualization of relationships across diverse protein superfamilies. *PLoS ONE* **2009**, *4*, e4345.
- 74. Ferrelli, M.L.; Pidre, M.L.; García-Domínguez, R.; Alberca, L.N.; del Saz-Navarro, D.; Santana-Molina, C.; Devos, D.P. Prokaryotic membrane coat-like proteins: An update. *J. Struct. Biol.* **2023**, 215, 107987. [CrossRef]
- 75. Zou, P.; Yang, X.; Yuan, Y.; Jing, C.; Cao, J.; Wang, Y.; Zhang, L.; Zhang, C.; Li, Y. Purification and characterization of a fucoidan from the brown algae *Macrocystis pyrifera* and the activity of enhancing salt-stress tolerance of wheat seedlings. *Int. J. Biol. Macromol.* **2021**, *180*, 547–558. [CrossRef]
- 76. Arijón, M.; Ponce, N.M.; Solana, V.; Dellatorre, F.G.; Latour, E.A.; Stortz, C.A. Monthly fluctuations in the content and monosaccharide composition of fucoidan from *Undaria pinnatifida* sporophylls from northern Patagonia. *J. Appl. Phycol.* **2021**, *33*, 2433–2441. [CrossRef]
- 77. Bilan, M.I.; Grachev, A.A.; Ustuzhanina, N.E.; Shashkov, A.S.; Nifantiev, N.E.; Usov, A.I. A highly regular fraction of a fucoidan from the brown seaweed *Fucus distichus* L. *Carbohydr. Res.* **2004**, *339*, 511–517. [CrossRef]
- 78. Silchenko, A.S.; Kusaykin, M.I.; Kurilenko, V.V.; Zakharenko, A.M.; Isakov, V.V.; Zaporozhets, T.S.; Gazha, A.K.; Zvyagintseva, T.N. Hydrolysis of fucoidan by fucoidanase isolated from the marine bacterium, *Formosa algae. Mar. Drugs* **2013**, *11*, 2413–2430.
- Silchenko, A.S.; Rasin, A.B.; Kusaykin, M.I.; Kalinovsky, A.I.; Miansong, Z.; Changheng, L.; Malyarenko, O.; Zueva, A.O.; Zvyagintseva, T.N.; Ermakova, S.P. Structure, enzymatic transformation, anticancer activity of fucoidan and sulphated fucooligosaccharides from Sargassum horneri. Carbohydr. Polym. 2017, 175, 654–660.
- 80. Satoh, T.; Sato, K.; Kanoh, A.; Yamashita, K.; Yamada, Y.; Igarashi, N.; Kato, R.; Nakano, A.; Wakatsuki, S. Structures of the carbohydrate recognition domain of Ca²⁺-independent cargo receptors Emp46p and Emp47p. *J. Biol. Chem.* **2006**, 281, 10410–10419. [CrossRef]
- 81. Sakka, M.; Kunitake, E.; Kimura, T.; Sakka, K. Function of a laminin_G_3 module as a carbohydrate-binding module in an arabinofuranosidase from *Ruminiclostridium josui*. *FEBS Lett.* **2019**, 593, 42–51.
- 82. Gupta, G.; Gupta, R.K.; Gupta, G. R-type lectin families. In *Animal Lectins: Form, Function and Clinical Applications*; Gupta, G.S., Ed.; Springer: Vienna, Austria, 2012; pp. 313–330.
- 83. Boraston, A.B.; Tomme, P.; Amandoron, E.A.; Kilburn, D.G. A novel mechanism of xylan binding by a lectin-like module from *Streptomyces lividans* xylanase 10A. *Biochem. J.* **2000**, *350*, 933–941.
- 84. Notenboom, V.; Boraston, A.B.; Williams, S.J.; Kilburn, D.G.; Rose, D.R. High-resolution crystal structures of the lectin-like xylan binding domain from *Streptomyces lividans* xylanase 10A with bound substrates reveal a novel mode of xylan binding. *Biochemistry* **2002**, *41*, 4246–4254. [CrossRef] [PubMed]
- 85. Ji, S.; Tian, X.; Li, X.; She, Q. Identification and structural analysis of a carbohydrate-binding module specific to alginate, a representative of a new family, CBM96. *J. Biol. Chem.* **2023**, 299, 102854. [CrossRef] [PubMed]
- 86. Wiegand, S.; Jogler, M.; Boedeker, C.; Pinto, D.; Vollmers, J.; Rivas-Marín, E.; Kohn, T.; Peeters, S.H.; Heuer, A.; Rast, P. Cultivation and functional characterization of 79 planctomycetes uncovers their unique biology. *Nat. Microbiol.* **2020**, *5*, 126–140. [CrossRef]
- 87. Friedlander, A.M.; Ballesteros, E.; Bell, T.W.; Caselle, J.E.; Campagna, C.; Goodell, W.; Hüne, M.; Muñoz, A.; Salinas-de-León, P.; Sala, E. Kelp forests at the end of the earth: 45 years later. *PLoS ONE* **2020**, *15*, e0229259. [CrossRef] [PubMed]
- 88. Mahadev, R.K.; Di Pietro, S.M.; Olson, J.M.; Piao, H.L.; Payne, G.S.; Overduin, M. Structure of Sla1p homology domain 1 and interaction with the NPFxD endocytic internalization motif. *EMBO J.* **2007**, *26*, 1963–1971. [PubMed]
- 89. Santarella-Mellwig, R.; Franke, J.; Jaedicke, A.; Gorjanacz, M.; Bauer, U.; Budd, A.; Mattaj, I.W.; Devos, D.P. The compartmentalized bacteria of the Planctomycetes-Verrucomicrobia-Chlamydiae superphylum have membrane coat-like proteins. *PLoS Biol.* **2010**, *8*, e1000281. [CrossRef]
- 90. Krause-Jensen, D.; Duarte, C.M. Substantial role of macroalgae in marine carbon sequestration. *Nat. Geosci.* **2016**, *9*, 737–742. [CrossRef]
- 91. Matos, M.N.; Lozada, M.; Anselmino, L.E.; Musumeci, M.A.; Henrissat, B.; Jansson, J.K.; Mac Cormack, W.P.; Carroll, J.; Sjöling, S.; Lundgren, L. Metagenomics unveils the attributes of the alginolytic guilds of sediments from four distant cold coastal environments. *Environ. Microbiol.* **2016**, *18*, 4471–4484. [CrossRef]
- 92. Ponce, N.M.; Stortz, C.A. A comprehensive and comparative analysis of the fucoidan compositional data across the Phaeophyceae. *Front. Plant Sci.* **2020**, *11*, 556312.

93. Amin, O.; Comoglio, L.; Spetter, C.; Duarte, C.; Asteasuain, R.; Freije, R.H.; Marcovecchio, J. Assessment of land influence on a high-latitude marine coastal system: Tierra del Fuego, southernmost Argentina. *Environ. Monit. Assess.* **2011**, *175*, 63–73. [PubMed]

- 94. Li, P.; Wang, S.; Samo, I.A.; Zhang, X.; Wang, Z.; Wang, C.; Li, Y.; Du, Y.; Zhong, Y.; Cheng, C. Common-ion effect triggered highly sustained seawater electrolysis with additional NaCl production. *Research* 2020, 2020, 872141. [CrossRef] [PubMed]
- 95. Niiranen, L.; Altermark, B.; Brandsdal, B.O.; Leiros, H.K.S.; Helland, R.; Smalås, A.O.; Willassen, N.P. Effects of salt on the kinetics and thermodynamic stability of endonuclease I from *Vibrio salmonicida* and *Vibrio cholerae*. *FEBS J.* **2008**, 275, 1593–1605. [CrossRef] [PubMed]
- 96. Wang, J.; Liu, Z.; Pan, X.; Wang, N.; Li, L.; Du, Y.; Li, J.; Li, M. Structural and biochemical analysis reveals catalytic mechanism of fucoidan lyase from *Flavobacterium* sp. SA-0082. *Mar. Drugs* **2022**, *20*, 533. [CrossRef] [PubMed]
- 97. Ropartz, D.; Marion, L.; Fanuel, M.; Nikolic, J.; Jam, M.; Larocque, R.; Ficko-Blean, E.; Michel, G.; Rogniaux, H. In-depth structural characterization of oligosaccharides released by GH107 endofucanase Mf FcnA reveals enzyme subsite specificity and sulfated fucan substructural features. *Glycobiology* **2022**, 32, 276–288. [CrossRef] [PubMed]
- 98. Arai, Y.; Shingu, Y.; Yagi, H.; Suzuki, H.; Ohshiro, T. Occurrence of different fucoidanase genes in *Flavobacterium* sp. SW and enzyme characterization. *J. Biosci. Bioeng.* **2022**, *134*, 187–194. [CrossRef]
- 99. Sichert, A.; Le Gall, S.; Klau, L.J.; Laillet, B.; Rogniaux, H.; Aachmann, F.L.; Hehemann, J.-H. Ion-exchange purification and structural characterization of five sulfated fucoidans from brown algae. *Glycobiology* **2021**, *31*, 352–357. [CrossRef]
- 100. Lorbeer, A.J.; Charoensiddhi, S.; Lahnstein, J.; Lars, C.; Franco, C.M.; Bulone, V.; Zhang, W. Sequential extraction and characterization of fucoidans and alginates from *Ecklonia radiata*, *Macrocystis pyrifera*, *Durvillaea potatorum*, and *Seirococcus axillaris*. *J. Appl. Phycol.* **2017**, 29, 1515–1526.
- 101. Zhang, W.; Oda, T.; Yu, Q.; Jin, J.-O. Fucoidan from *Macrocystis pyrifera* has powerful immune-modulatory effects compared to three other fucoidans. *Mar. Drugs* **2015**, *13*, 1084–1104. [CrossRef]
- 102. Koh, H.S.A.; Lu, J.; Zhou, W. Structure characterization and antioxidant activity of fucoidan isolated from *Undaria pinnatifida* grown in New Zealand. *Carbohydr. Polym.* **2019**, 212, 178–185. [CrossRef] [PubMed]
- 103. Liuzzi, M.G.; López Gappa, J.; Piriz, M.L. Latitudinal gradients in macroalgal biodiversity in the Southwest Atlantic between 36 and 55 S. *Hydrobiologia* **2011**, 673, 205–214. [CrossRef]

Disclaimer/Publisher's Note: The statements, opinions and data contained in all publications are solely those of the individual author(s) and contributor(s) and not of MDPI and/or the editor(s). MDPI and/or the editor(s) disclaim responsibility for any injury to people or property resulting from any ideas, methods, instructions or products referred to in the content.